



ELSEVIER

Contents lists available at ScienceDirect

Journal of Computational Physics

www.elsevier.com/locate/jcp



Numerical methods for high-dimensional probability density function equations

H. Cho^a, D. Venturi^c, G.E. Karniadakis^{b,*}^a Department of Mathematics, University of Maryland College Park, College Park, MD 20742, USA^b Division of Applied Mathematics, Brown University, Providence, RI 02912, USA^c Department of Applied Mathematics and Statistics, University of California Santa Cruz, Santa Cruz, CA 95064, USA

ARTICLE INFO

Article history:

Received 17 October 2014

Received in revised form 20 October 2015

Accepted 22 October 2015

Available online 10 November 2015

Keywords:

High-order numerical methods
 Proper generalized decomposition
 Uncertainty quantification
 Stochastic dynamical systems
 Kinetic partial differential equations
 ANOVA decomposition

ABSTRACT

In this paper we address the problem of computing the numerical solution to kinetic partial differential equations involving many phase variables. These types of equations arise naturally in many different areas of mathematical physics, e.g., in particle systems (Liouville and Boltzmann equations), stochastic dynamical systems (Fokker–Planck and Dostupov–Pugachev equations), random wave theory (Malakhov–Saichev equations) and coarse-grained stochastic systems (Mori–Zwanzig equations). We propose three different classes of new algorithms addressing high-dimensionality: The first one is based on separated series expansions resulting in a sequence of low-dimensional problems that can be solved recursively and in parallel by using alternating direction methods. The second class of algorithms relies on truncation of interaction in low-orders that resembles the Bogoliubov–Born–Green–Kirkwood–Yvon (BBGKY) framework of kinetic gas theory and it yields a hierarchy of coupled probability density function equations. The third class of algorithms is based on high-dimensional model representations, e.g., the ANOVA method and probabilistic collocation methods. A common feature of all these approaches is that they are reducible to the problem of computing the solution to high-dimensional equations via a sequence of low-dimensional problems. The effectiveness of the new algorithms is demonstrated in numerical examples involving nonlinear stochastic dynamical systems and partial differential equations, with up to 120 variables.

© 2015 Elsevier Inc. All rights reserved.

1. Introduction

Kinetic equations are partial differential equations involving probability density functions (PDFs). They arise naturally in many different areas of mathematical physics. For example, they play an important role in modeling rarefied gas dynamics [1,2], semiconductors [3], stochastic dynamical systems [4–10], structural dynamics [11–13], stochastic partial differential equations (PDEs) [14–18], turbulence [19–22], system biology [23–25], etc. Perhaps, the most well-known kinetic equation is the Fokker–Planck equation [4,26,27], which describes the evolution of the probability density function of Langevin-type dynamical systems subject to Gaussian white noise. Another well-known example of kinetic equation is the Boltzmann equation [28] describing a thermodynamic system involving a large number of interacting particles [2]. Other examples that are may not be widely known are the Dostupov–Pugachev equations [7,10,11,29], the reduced-order Nakajima–Zwanzig–

* Corresponding author.

E-mail address: gk@dam.brown.edu (G.E. Karniadakis).

Table 1
Examples of kinetic equations arising in different areas of mathematical physics.

Fokker–Planck [26,4]	$\frac{\partial p}{\partial t} + \sum_{i=1}^n \frac{\partial}{\partial z_i} (G_i p) = \frac{1}{2} \sum_{i,j=1}^n \frac{\partial^2}{\partial z_i \partial z_j} (b_{ij} p)$
Boltzmann [1,31]	$\frac{\partial p}{\partial t} + \sum_{k=1}^3 v_k \frac{\partial p}{\partial z_k} = H(p, p)$
Liouville [7,15,29,11]	$\frac{\partial p}{\partial t} + \sum_{k=1}^n \frac{\partial}{\partial z_k} (G_k p) = 0$
Malakhov–Saichev [17,14]	$\frac{\partial p}{\partial t} + \frac{\partial}{\partial z} \left(\sum_{k=1}^3 G_k \int_{-\infty}^z \frac{\partial p}{\partial x_k} dz' \right) = -\frac{\partial (Hp)}{\partial z}$
Mori–Zwanzig [30,16]	$\frac{\partial p_1}{\partial t} = PLp_1 + PL e^{tQL} p_2(0) + PL \int_0^t e^{(t-s)QL} QL p_1 ds$

Mori equations [16,30], and the Malakhov–Saichev PDF equations [17,14] (see Table 1). Computing the numerical solution to a kinetic equation is a very challenging task that involves several problems of different nature:

1. *High-dimensionality*: Kinetic equations describing realistic physical systems usually involve many phase variables. For example, the Fokker–Planck equation of classical statistical mechanics yields a joint probability density function in n phase variables, where n is the dimension of the underlying stochastic dynamical system, plus time.
2. *Multiple scales*: Kinetic equations can involve multiple scales in space and time, which could be hardly accessible by conventional numerical methods. For example, the Liouville equation is a hyperbolic conservation law whose solution is purely advected (with no diffusion) by the underlying system’s flow map. This can easily yield mixing, fractal attractors, and all sorts of complex dynamics.
3. *Lack of regularity*: The solution to a kinetic equation is, in general, a distribution [32]. For example, it could be a multi-variate Dirac delta function, a function with shock-type discontinuities [18], or even a fractal object (see Fig. 1 in [16]). From a numerical viewpoint, resolving such distributions is not trivial although in some cases it can be done by taking integral transformations or projections [33].
4. *Conservation properties*: There are several properties of the solution to a kinetic equation that must be conserved in time. The most obvious one is mass, i.e., the solution to a kinetic equation always integrates to one. Another property that must be preserved is the positivity of the joint PDF, and the fact that a partial marginalization still yields a PDF.
5. *Long-term integration*: The flow map defined by nonlinear dynamical systems can yield large deformations, stretching and folding of the phase space. As a consequence, numerical schemes for kinetic equations associated with such systems will generally lose accuracy in time. This is known as long-term integration problem and it can be eventually mitigated by using adaptive methods.

Over the years, many different techniques have been proposed to address these issues, with the most efficient ones being problem-dependent. For example, a widely used method in statistical fluid mechanics is the particle/mesh method [22,34–36], which is based directly on stochastic Lagrangian models. Other methods make use of stochastic fields [37] or direct quadrature of moments [38]. In the case of Boltzmann equation, there is a very rich literature. Both probabilistic approaches such as direct simulation Monte Carlo [39,40], as well as deterministic methods, e.g., discontinuous Galerkin and spectral methods [41–43], have been proposed to compute the solution. Probabilistic methods such as direct Monte Carlo are extensively used because of their very low computational cost compared to finite-volumes, finite-differences or spectral methods, especially in the multi-dimensional case. However, Monte Carlo usually yields poorly accurate and fluctuating solutions, which need to be post-processed appropriately, for example through variance reduction techniques. We refer to Dimarco and Pareschi [31] for a recent review.

In our previous work [9], we addressed the lack of regularity and high-dimensionality (in the space of parameters) of kinetic equations by using adaptive discontinuous Galerkin methods [44,45] combined with sparse probabilistic collocation. Specifically, the phase variables of the system were discretized by using spectral elements on an adaptive non-conforming grid that track the support of the PDF in time, while the parametric dependence of the solution was handled by using sparse grids. However, the discontinuous Galerkin method we proposed in [9] is effective for phase spaces of dimension not exceeding three.

In this paper, we address the high-dimensional challenge in both of the *phase space* and *parametric space* by using different techniques, i.e., separated series expansion methods, Bogoliubov–Born–Green–Kirkwood–Yvon (BBGKY) closures, and analysis of variance (ANOVA) approximations. The key idea of separated representations is to approximate a multi-dimensional function in terms of series involving products of one-dimensional functions [46–49]. As we will see, this allows us to reduce the problem of computing the solution from high-dimensional kinetic equations to a sequence of one-dimensional problems that can be solved recursively and in parallel by using alternating direction algorithms, e.g., alternating least squares. The convergence rate of these algorithms with respect to the number of terms in the series expansion

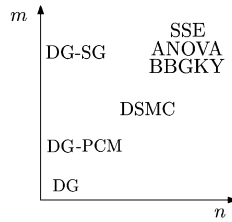


Fig. 1. Range of applicability of different numerical methods for solving kinetic equations as a function of the number of phase variables n and the number of parameters m appearing in the equation. Shown in the upper right are: Separated series expansion methods (SSE – section 2.1), BBGKY closures (BBGKY – section 2.2), high-dimensional model representations (ANOVA – section 2.3), adaptive discontinuous Galerkin methods (DG) with sparse grids (SG) or tensor product probabilistic collocation (PCM) in the parameter space, direct simulation Monte Carlo (DSMC).

sion strongly depends on the kinetic equation as well as on its solution. For example, advection-dominated equations yield a rather slow convergence rate¹ [49]. Alongside separated representation, we also investigate BBGKY type closures that rely on truncation of interaction in low-orders. Such an approach developed in kinetic gas theory [50] yields a hierarchy of coupled PDF equations for a given stochastic dynamical system. The third approach we consider is based on ANOVA approximation methods [51–54]. The basic idea is to represent multivariate PDFs in terms of series expansions involving functions with a smaller number of variables. For example, a second-order ANOVA approximation of a multivariate PDF in N variables² is a series involving functions of at most two variables. All of these methods allow us to reduce the problem of computing high-dimensional PDF solutions to a sequence of problems involving low-dimensional PDFs. The range of applicability the proposed new approaches as well as and other numerical methods is sketched in Fig. 1 as a function of the number of phase variables n and the number of parameters m appearing in the kinetic equation.

This paper is organized as follows. In section 2, we present three different classes of new algorithms to solve high-dimensional kinetic equations, i.e., the separated series expansion method (section 2.1), the BBGKY closure approximation (section 2.2), and the ANOVA series expansion method (section 2.3). The computational cost of these algorithms is discussed in section 3. In section 4, we apply the proposed new techniques to kinetic equations arising in nonlinear stochastic dynamical system theory (Kraichnan–Orszag and Lorenz-96 systems) as well as to stochastic partial differential equations (random advection and random diffusion problems). Finally, the main findings are summarized in section 5. We also include a brief appendix dealing with the finite-dimensional representation of the alternating-direction Galerkin algorithms we propose in section 2.1.

2. Numerical methods

In this section we present three classes of algorithms to compute the numerical solution of high-dimensional kinetic equations, such as those summarized in Table 1. The first class is based on separated series expansions (SSE) and alternating direction methods. The second class of algorithms relies on the BBGKY type approximation (BBGKY) and it yields a hierarchy of coupled probability density function equations. The third class is based on high-dimensional model representations (ANOVA) and probabilistic collocation methods. Hereafter we describe each method in detail.

2.1. Separated series expansions (SSE)

The method of separation of variables has been widely used to approximate high-dimensional functions in terms of low-dimensional ones. In particular, let us consider the following separated expansion of an N -dimensional probability density function

$$p(z_1, \dots, z_N) = \sum_{r=1}^R \alpha_r p_1^r(z_1) p_2^r(z_2) \cdots p_N^r(z_N) + \epsilon(z_1, \dots, z_N), \tag{1}$$

where R is the *separation rank*, p_j^r are one-dimensional functions, and ϵ is the residual. The total number of variables N in equation (1) is the sum of the phase variables n and the number of parameters m appearing in the kinetic equation. Specific examples will be given in section 4. The main advantage of using a representation in the form (1) to solve a high-dimensional kinetic PDE relies on the fact that the algorithms to compute $p_j^r(z_j)$ and the normalization factors α_r involve operations with one function at a time. Thus, in principle, the computational cost of such algorithms grows linearly with respect to the dimension N , potentially avoiding the curse of dimensionality.

¹ The Liouville equation is a hyperbolic conservation law in which the diffusion term is completely absent (see Table 1). Therefore, the convergence rate of the separated representation of the solution is usually quite slow. On the other hand, fast convergence was observed for Fokker–Planck equations by Leonenko and Phillips [47].

² In this paper, the total number of variables N is the sum of the number of phase variables n and the number of parameters m appearing in the kinetic equation, i.e., $N = n + m$.

For time-dependent PDEs, we can still look for solutions in the form (1), where we simply add additional functions of the time variable in the separated series. This approach has been considered by several authors, e.g., [46,55], and it was shown to work well for problems dominated by diffusion. However, for complex transient problems (e.g., hyperbolic dynamics), such an approach is not practical as it requires a high resolution in time domain. To address this issue, a discontinuous Galerkin method in time was proposed by Nouy in [49]. The key idea is to split the integration period into small intervals (finite elements in time) and then consider a space–time separated representation of the solution within each interval. In this paper we follow a different approach, based on explicit or implicit time-integration schemes. In this case, the separated representation of the solution is computed at each time step. Let us formulate the method with reference to a linear kinetic equation in the form

$$\frac{\partial p(\mathbf{z}, t)}{\partial t} = L(\mathbf{z})p(\mathbf{z}, t), \tag{2}$$

where $\mathbf{z} = (z_1, \dots, z_N)$ is the vector of phase variables and $L(\mathbf{z})$ is a linear operator. For instance, in the case of the Fokker–Planck equation (see Table 1) we have $m = 0$ (i.e. $N = n$) and

$$L(\mathbf{z}) = - \sum_{k=1}^n \left(\frac{\partial G_k(\mathbf{z})}{\partial z_k} - G_k(\mathbf{z}) \frac{\partial}{\partial z_k} \right) + \frac{1}{2} \sum_{i,j=1}^n \left(\frac{\partial^2 b_{ij}(\mathbf{z})}{\partial z_i \partial z_j} + b_{ij}(\mathbf{z}) \frac{\partial^2}{\partial z_i \partial z_j} \right).$$

The time-discrete version of (2) can be easily obtained by applying, e.g., the Crank–Nicolson scheme. This yields

$$\frac{p(\mathbf{z}, t_{j+1}) - p(\mathbf{z}, t_j)}{\Delta t} = \frac{1}{2} (L(\mathbf{z})p(\mathbf{z}, t_{j+1}) + L(\mathbf{z})p(\mathbf{z}, t_j)), \quad \Delta t = t_{j+1} - t_j,$$

i.e.,

$$\left(I - \frac{1}{2} \Delta t L(\mathbf{z}) \right) p(\mathbf{z}, t_{j+1}) = \left(I + \frac{1}{2} \Delta t L(\mathbf{z}) \right) p(\mathbf{z}, t_j). \tag{3}$$

Assuming that $p(\mathbf{z}, t_j)$ is known, (3) is a linear equation for $p(\mathbf{z}, t_{j+1})$ which can be written concisely as³

$$A(\mathbf{z}) p(\mathbf{z}) = f(\mathbf{z}), \tag{4}$$

where

$$A(\mathbf{z}) \doteq \left(I - \frac{1}{2} \Delta t L(\mathbf{z}) \right), \quad f(\mathbf{z}) \doteq \left(I + \frac{1}{2} \Delta t L(\mathbf{z}) \right) p(\mathbf{z}, t_j). \tag{5}$$

The system operator $A(\mathbf{z})$ and the right-hand-side $f(\mathbf{z})$ are assumed to be separable with respect to \mathbf{z} , i.e.,

$$A(\mathbf{z}) = \sum_{k=1}^{n_A} A_1^k(z_1) \cdots A_N^k(z_N), \quad f(\mathbf{z}) = \sum_{k=1}^{n_f} f_1^k(z_1) \cdots f_N^k(z_N). \tag{6}$$

Note that $A(\mathbf{z})$ is separable if $L(\mathbf{z})$ is separable. An example is the Liouville operator associated with the Kraichnan–Orszag problem (see subsequent equations (18a)–(18c) and (19))

$$L(\mathbf{z}) = -z_1 z_2 \frac{\partial}{\partial z_1} - z_2 z_3 \frac{\partial}{\partial z_2} - (z_2^2 - z_1^2) \frac{\partial}{\partial z_3} - (z_2 + z_3). \tag{7}$$

More generally, systems with polynomial-type nonlinearities always yield separable Liouvillians $L(\mathbf{z})$, and therefore separable $A(\mathbf{z})$. At this point, we look for a separated representation of the solution to (4) in the form

$$p^R(\mathbf{z}) = \sum_{r=1}^R \alpha_r p_1^r(z_1) \cdots p_N^r(z_N), \tag{8}$$

and we try to determine α_r , p_j^r and the separation rank R based on the condition

$$\|A(\mathbf{z})p^R(\mathbf{z}) - f(\mathbf{z})\| \leq \varepsilon, \tag{9}$$

in an appropriately chosen norm, and for a prescribed target accuracy ε . This problem does not admit a unique solution. In fact, there exist many possible choices of α_r , $p_j^r(z_j)$ and R that yield, in norm, the same target accuracy. Hence, different approaches exist to compute $p_j^r(z_j)$ and α_r . Hereafter, we focus our attention on alternating-direction Galerkin and least squares methods.

³ Note that in equation (4) we have omitted the time-dependence in $p(\mathbf{z}, t_{j+1})$ for notational convenience.

Alternating direction algorithms

The basic idea of alternating direction methods is to construct the series expansion (8) iteratively, by determining $p_j^r(z_j)$ one at a time while freezing all other functions. This yields a sequence of low-dimensional problems that can be solved efficiently and in parallel [46–49,56–58]. To clarify how the method works in simple terms, suppose we have constructed an approximated solution to (4) in the form (8), i.e., suppose we have available $p^R(\mathbf{z})$. Then we look for an enriched solution in the form

$$p^R(\mathbf{z}) + r_1(z_1) \cdots r_N(z_N),$$

where $\{r_1(z_1), \dots, r_N(z_N)\}$ are N unknown functions to be determined. In the alternating direction method, such functions are determined iteratively, one at a time. Typical algorithms to perform such iterations are based on least squares,

$$\min_{r_j} \left\| \sum_{k=1}^{n_A} A_1^k \cdots A_N^k (p^R + r_1 \cdots r_N) - \sum_{k=1}^{n_f} f_1^k \cdots f_N^k \right\|^2, \tag{10}$$

or Galerkin methods

$$\left\langle q, \sum_{k=1}^{n_A} A_1^k \cdots A_N^k (p^R + r_1 \cdots r_N) \right\rangle = \left\langle q, \sum_{k=1}^{n_f} f_1^k \cdots f_N^k \right\rangle, \tag{11}$$

where $\langle \cdot \rangle$ is an inner product (multi-dimensional integral with respect to \mathbf{z}), and q is a test function, often chosen as $q(\mathbf{z}) = r_1(z_1) \cdots r_N(z_N)$. In a finite-dimensional setting, the minimization problem (10) reduces to the problem of finding the minimum of a scalar function in as many variables as the number of unknowns we consider in each basis function $r_j(z_j)$, say q_z . Similarly, the alternating-direction solution to (11) is based on the iterated solution to a sequence of low-dimensional linear systems of size $q_z \times q_z$. Note that if $A(\mathbf{z})$ in Eq. (4) is a nonlinear operator, then we can still solve (10) or (11), e.g., by using Newton iterations. Once the functions $\{r_1(z_1), \dots, r_N(z_N)\}$ are computed, they are normalized (yielding the normalization factor α_{R+1}) and added to $p^R(\mathbf{z})$ to obtain $p^{R+1}(\mathbf{z})$. The separation rank is increased until (9) is satisfied for a desired target accuracy ε .

The enrichment procedure just described has been criticized in the literature due to its slow convergence, in particular for equations dominated by advection [49]. Depending on the criterion used to construct the separated expansion, the enrichment procedure might not even converge. Recent work, indeed, aimed at finding optimal bases with granted convergence properties, i.e., bases that minimize the separation rank and simultaneously keep the overall error (9) bounded by ε . For example, Doostan and Iaccarino [59] proposed an alternating least-square algorithm that updates simultaneously the entire rank of the basis set in the j -th direction. In this formulation, the least square approach (10) becomes

$$\min_{\{p_1^1, \dots, p_j^R\}} \left\| \sum_{k=1}^{n_A} A_1^k \cdots A_N^k \left(\sum_{r=1}^R \alpha_r p_1^r \cdots p_N^r \right) - \sum_{k=1}^{n_f} f_1^k \cdots f_N^k \right\|^2.$$

The computational cost of this method clearly increases compared to (10). In fact, in a finite dimensional setting, the simultaneous determination of $\{p_j^1, \dots, p_j^R\}$ requires the solution of a $Rq_z \times Rq_z$ linear system, where q_z is the number of degrees of freedom for each $p_j^r(z_j)$. However, this algorithm usually results in a separated solution with a lower separation rank R than the regular approach.

Hereafter, we propose a new alternating direction Galerkin method that, as before, updates the entire rank of the basis set in the j -th phase variable simultaneously. To this end, we generalize the Galerkin formulation (11) to

$$\left\langle q, \sum_{k=1}^{n_A} A_1^k \cdots A_N^k \left(\sum_{r=1}^R \alpha_r p_1^r \cdots p_N^r \right) \right\rangle = \left\langle q, \sum_{k=1}^{n_f} f_1^k \cdots f_N^k \right\rangle, \tag{12}$$

where $q(\mathbf{z}) = \text{span}\{p_1^r(z_1) \cdots p_N^r(z_N)\}_{r=1}^R$. In addition, we employ an adaptive strategy to determine the separation rank based on the spectrum $\alpha = \{\alpha_1, \dots, \alpha_R\}$ of the separated series. The adaptive criterion is simple and effective:

- We increase the separation rank R if the ratio α_R/α_1 exceeds a threshold θ .

The finite-dimensional representation of (12) and the summary of the algorithm is discussed in Appendix A and Table 3, respectively.

2.2. BBGKY closures

In addition to the separated series expansion method discussed in the previous section, we propose here a BBGKY type closure to further reduce the dimensionality of a kinetic equation. Let us introduce the method with reference to a nonlinear dynamical system in the form

$$\frac{d\mathbf{x}(t)}{dt} = \mathbf{Q}(\mathbf{x}, \boldsymbol{\xi}, t), \quad \mathbf{x}(0) = \mathbf{x}_0(\omega), \quad (13)$$

where $\mathbf{x}(t) \in \mathbb{R}^n$ is a multi-dimensional stochastic process, $\boldsymbol{\xi} \in \mathbb{R}^m$ is a vector of random variables, $\mathbf{Q}: \mathbb{R}^{n+m+1} \rightarrow \mathbb{R}^n$ is a Lipschitz continuous (deterministic) function, and $\mathbf{x}_0 \in \mathbb{R}^n$ is a random initial state. Upon definition of $\mathbf{y}(t) = (\mathbf{x}(t), \boldsymbol{\xi})$, we can rewrite (13) as

$$\frac{d\mathbf{y}(t)}{dt} = \mathbf{G}(\mathbf{y}, t), \quad \mathbf{y}(0) = (\mathbf{x}_0(\omega), \boldsymbol{\xi}(\omega)), \quad \mathbf{G}(\mathbf{y}, t) = \begin{bmatrix} \mathbf{Q}(\mathbf{y}, t) \\ \mathbf{0} \end{bmatrix}. \quad (14)$$

Note that $\mathbf{y}(t) \in \mathbb{R}^N$ and $\mathbf{G}: \mathbb{R}^{N+1} \rightarrow \mathbb{R}^N$, where $N = n + m$. The joint PDF of $\mathbf{y}(t)$ evolves according to the Liouville equation

$$\frac{\partial p(\mathbf{z}, t)}{\partial t} + \nabla \cdot [\mathbf{G}(\mathbf{z}, t)p(\mathbf{z}, t)] = 0, \quad \mathbf{z} \in \mathbb{R}^N, \quad (15)$$

whose solution can be computed numerically only for small N . This leads us to look for PDF equations involving only a reduced number of phase variables, for instance, the PDF of each component $y_i(t)$. The derivation relies on the functional integral form of the PDF $p_{\mathbf{y}}(\mathbf{z}, t) = \int \prod_{i=1}^N \delta(z_i - y_i(\mathbf{x}_0, \boldsymbol{\xi}; t)) w(\mathbf{x}_0, \boldsymbol{\xi}) d\mathbf{x}_0 d\boldsymbol{\xi}$, where $w(\mathbf{x}_0, \boldsymbol{\xi})$ is the joint PDF of the initial random variables and the parameters \mathbf{x}_0 and $\boldsymbol{\xi}$. Then, by differentiating both sides with respect to t , the PDF of a single component $y_i(t)$ satisfies⁴

$$\begin{aligned} \frac{\partial p_i(z_i, t)}{\partial t} &= -\frac{\partial}{\partial z_i} \int [\dot{y}_i(t) \delta(z_i - y_i(t)) w(\mathbf{x}_0, \boldsymbol{\xi})] d\mathbf{x}_0 d\boldsymbol{\xi} \\ &= -\frac{\partial}{\partial z_i} \int [G_i(\mathbf{y}, t) \delta(z_i - y_i(t)) p(\mathbf{y}, t)] d\mathbf{y} \end{aligned} \quad (16)$$

where $p(\mathbf{y}, t)$ is the full joint PDF of $\mathbf{y}(t)$. Similarly, the joint PDF of $y_i(t)$ and $y_j(t)$ ($i \neq j$) satisfies

$$\begin{aligned} \frac{\partial p_{ij}(z_i, z_j, t)}{\partial t} &= -\frac{\partial}{\partial z_i} \int [G_i(\mathbf{y}, t) \delta(z_i - y_i(t)) \delta(z_j - y_j(t)) p(\mathbf{y}, t)] d\mathbf{y} \\ &\quad -\frac{\partial}{\partial z_j} \int [G_j(\mathbf{y}, t) \delta(z_i - y_i(t)) \delta(z_j - y_j(t)) p(\mathbf{y}, t)] d\mathbf{y}. \end{aligned} \quad (17)$$

Higher-order PDF equations can be derived similarly. Unfortunately, the computation of the integrals in (16) and (17) requires the full joint PDF of $\mathbf{y}(t)$, which is available only if we solve the Liouville equation (15). As mentioned before, this is not feasible in practice even for a low number of variables. Therefore, we need to introduce approximations. The most common one is to assume that the joint PDF $p(\mathbf{z}, t)$ can be written in terms of lower-order PDFs, e.g., as $p(\mathbf{z}, t) = p_1(z_1, t) \cdots p_N(z_N, t)$. By using integration by parts, this assumption reduces the Liouville equation to a hierarchy of one-dimensional PDF equations (see, e.g., [16]).

Hereafter we follow a similar approach based on lower order PDFs at least in second order. The idea is to approximate the dynamics in the i -th direction by primarily using the correlation to the i -th variable. If G_i is a function of z_i and z_j , the right-hand-side of (17) becomes

$$-\frac{\partial}{\partial z_i} \int [G_i(\mathbf{y}, t) \delta(z_i - y_i(t)) \delta(z_j - y_j(t)) p(\mathbf{y}, t)] d\mathbf{y} = -\frac{\partial}{\partial z_i} [G_i(z_i, z_j, t) p_{ij}(z_i, z_j, t)].$$

Otherwise, we approximate the equation by using the joint PDFs $p_{ik}(z_i, z_k)$ for $k \neq i$. To this end, let us consider a specific form of G_i that allows us to simplify the equations, i.e.,

$$G_i(\mathbf{y}, t) = g_{ii}(y_i, t) + \sum_{\substack{k=1 \\ k \neq i}}^N g_{ik}(y_i, y_k, t).$$

The integrals in the right hand side of the one-point PDF equation (16) can be now computed exactly as

$$\frac{\partial p_i}{\partial t} = -\frac{\partial}{\partial z_i} \left[g_{ii}(z_i, t) p_i + \sum_{k \neq i} \int g_{ik}(z_i, z_k, t) p_{ik} dz_k \right],$$

⁴ Note that $p_i(z_i, t) = p(\xi_i)$ for all $n+1 \leq i \leq n+m$, and for all $t \geq 0$.

where $p_i = p(z_i, t)$ and $p_{ik} = p(z_i, z_k, t)$. On the other hand, we approximate the integrals in the two-points PDF equations (17) as

$$\begin{aligned} \frac{\partial p_{ij}}{\partial t} = & -\frac{\partial}{\partial z_i} \left[(g_{ii}(z_i, t) + g_{ij}(z_i, z_j, t)) p_{ij} + \left(\sum_{k \neq i, j}^N \int g_{ik}(z_i, z_k, t) p_{ik} dz_k \right) p_j \right] \\ & -\frac{\partial}{\partial z_j} \left[(g_{jj}(z_j, t) + g_{ji}(z_j, z_i, t)) p_{ij} + \left(\sum_{k \neq i, j}^N \int g_{jk}(z_j, z_k, t) p_{jk} dz_k \right) p_i \right], \end{aligned}$$

where we discarded all contributions from the three-points PDFs and the two-points PDFs except the ones interacting with the i -th variable. A variance-based sensitivity analysis in terms of Sobol indices [60–62] can be performed to identify the system variables with strong correlations. This allows us to determine whether it is necessary to add the other two-points correlations or the three-points PDF equations for a certain triple $\{x_k(t), x_i(t), x_j(t)\}$, and to further determine the equation for a general form of G_i .

An example: the Kraichnan–Orszag problem

Let us apply the BBGKY type closure we described in the previous section to the Kraichnan–Orszag problem studied in [63]

$$\frac{dx_1}{dt} = x_1 x_3, \tag{18a}$$

$$\frac{dx_2}{dt} = -x_2 x_3, \tag{18b}$$

$$\frac{dx_3}{dt} = -x_1^2 + x_2^2. \tag{18c}$$

In this case we have $n = 3$ phase variables and $m = 0$ parameters, i.e., a total number of $N = 3$ variables. The three-dimensional Liouville equation for the joint PDF of $\{x_1(t), x_2(t), x_3(t)\}$, is

$$\frac{\partial p}{\partial t} + z_1 z_2 \frac{\partial p}{\partial z_1} - z_2 z_3 \frac{\partial p}{\partial z_2} + (z_2^2 - z_1^2) \frac{\partial p}{\partial z_3} = (-z_2 + z_3) p, \tag{19}$$

where $p = p(z_1, z_2, z_3, t)$. On the other hand, by using the second-order BBGKY closure described in the previous section, we obtain the following hierarchy of PDF equations

$$\frac{\partial p_1}{\partial t} = -\frac{\partial}{\partial z_1} [z_1 \langle x_3 \rangle_{3|1}], \tag{20a}$$

$$\frac{\partial p_2}{\partial t} = -\frac{\partial}{\partial z_2} [-z_2 \langle x_3 \rangle_{3|2}], \tag{20b}$$

$$\frac{\partial p_3}{\partial t} = -\frac{\partial}{\partial z_3} [(-\langle x_1^2 \rangle_{1|3} + \langle x_2^2 \rangle_{2|3})], \tag{20c}$$

$$\frac{\partial p_{12}}{\partial t} = -\frac{\partial}{\partial z_1} [z_1 \langle x_3 \rangle_{3|1} p_2] + \frac{\partial}{\partial z_2} [z_2 \langle x_3 \rangle_{3|2} p_1], \tag{20d}$$

$$\frac{\partial p_{13}}{\partial t} = -\frac{\partial}{\partial z_1} [z_1 z_3 p_{13}] + \frac{\partial}{\partial z_3} [z_1^2 p_{13} - \langle x_2^2 \rangle_{2|3} p_1], \tag{20e}$$

$$\frac{\partial p_{23}}{\partial t} = \frac{\partial}{\partial z_2} [z_2 z_3 p_{23}] + \frac{\partial}{\partial z_3} [\langle x_1^2 \rangle_{1|3} p_2 - z_2^2 p_{23}], \tag{20f}$$

where

$$\langle f(\mathbf{x}) \rangle_{i|j} \doteq \int f(\mathbf{z}) p_{ij}(z_i, z_j, t) dz_i. \tag{21}$$

Let us assess the accuracy of the second-order BBGKY closure (20a)–(20f) when the initial condition $\{x_1(0), x_2(0), x_3(0)\}$ is jointly Gaussian

$$p(z_1, z_2, z_3, t = 0) = \frac{10^3}{(2\pi)^{3/2}} \exp \left[-50 \left(z_1 - \frac{1}{10} \right)^2 - 50 \left(z_2^2 + z_3^2 \right) \right]. \tag{22}$$

Each PDF equation is discretized by using a Fourier spectral collocation method with $q_z = 50$ degrees of freedom in each variable. Time stepping is based on explicit fourth-order Runge–Kutta scheme with $\Delta t = 10^{-3}$. In Fig. 2, we compare the PDF of $x_1(t)$ and $x_2(t)$ as computed by the full system and the two-points BBGKY closure. We observe that the two solutions

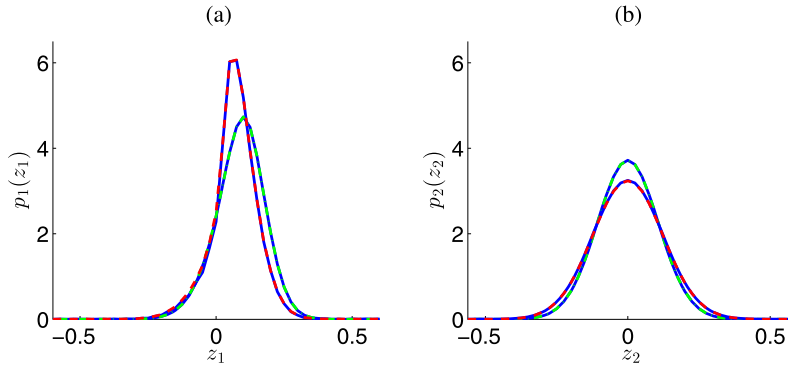


Fig. 2. Kraichnan–Orszag problem: PDF of $x_1(t)$ (a) and $x_2(t)$ (b) at $t = 4$ and $t = 8$. Blue lines: results from the full Liouville equation. Green and red dashed line: results of the BBGKY closure (20a)–(20f) at $t = 4$ and $t = 8$, respectively. (For interpretation of the references to color in this figure legend, the reader is referred to the web version of this article.)

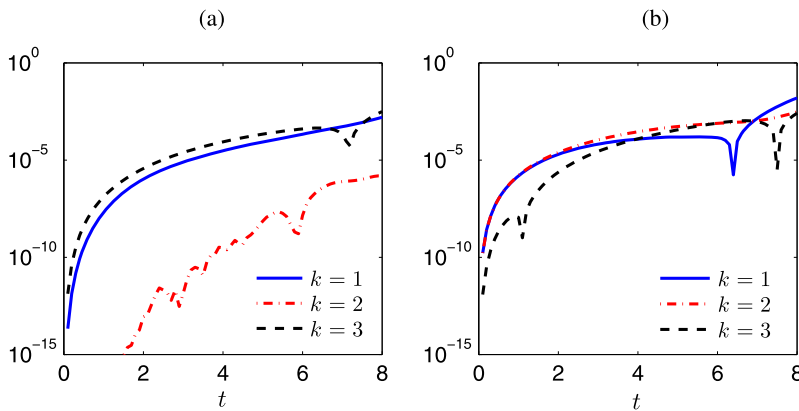


Fig. 3. Kraichnan–Orszag problem: Absolute error in the mean (a) and in the standard deviation (b) of $x_k(t)$ ($k = 1, 2, 3$) computed by the two-points BBGKY closure (20a)–(20f).

are basically superimposed, suggesting that the effects of the three-points correlations are negligible. We also remark that if we are interested only in the PDF of one variable, then it is not necessary to solve the whole hierarchy of PDF equations in the BBGKY closure. For example, to obtain the PDF of $x_1(t)$, we can just solve Eqs. (20a), (20e), and (20f). In Fig. 3, we plot the absolute error in the mean and the standard deviation of $\{x_1(t), x_2(t), x_3(t)\}$ as computed by the BBGKY closure. These errors arise because we are not including the three-points PDFs in the hierarchy of equations.

We also emphasize that the PDF equation of a phase space function $h(x_1, x_2, x_3)$, can be easily derived based on the BBGKY closure. For example, the PDF equation of $h = x_1(t) + x_3(t)$ is

$$\frac{\partial p_h(z)}{\partial t} = -\frac{\partial}{\partial z} \left[\left(-z^2 + 3z\langle x_3 \rangle_{3|h} - 2\langle x_3^2 \rangle_{3|h} + \langle x_2^2 \rangle_{2|h} \right) p_h(z) \right].$$

2.3. ANOVA series expansions

The ANOVA series expansion [53,64] is another typical approach to model high-dimensional functions. The series involves a superimposition of functions with an increasing number of variables, and it is usually truncated at a certain interaction order. Specifically, the ANOVA expansion of an N -dimensional PDF takes the form [65]

$$p(z_1, z_2, \dots, z_N) = q_0 + \sum_{i=1}^N q_i(z_i) + \sum_{i<j}^N q_{ij}(z_i, z_j) + \sum_{i<j<k}^N q_{ijk}(z_i, z_j, z_k) + \dots \tag{23}$$

The function q_0 is a constant. The functions $q_i(z_i)$, which we shall call first-order interaction terms, give us the overall effects of the variables z_i in p as if they were acting independently of the other variables. The functions $q_{ij}(z_i, z_j)$ describe the interaction effects of the variables z_i and z_j , and therefore they will be called second-order interactions. Similarly, higher-order terms reflect the cooperative effects of an increasing number of variables. The interaction terms $q_{ijk} \dots$ can be computed in different ways [66,67], e.g.,

$$\begin{aligned}
 q_0 &= \int p(z_1, \dots, z_N) dz_1, \dots, dz_N, \\
 q_i(z_i) &= \int p(z_1, \dots, z_N) \prod_{\substack{k=1 \\ k \neq i}}^N dz_k - q_0, \\
 q_{ij}(z_i, z_j) &= \int p(z_1, \dots, z_N) \prod_{\substack{k=1 \\ k \neq i, j}}^N dz_k - q_0 - q_i(z_i) - q_j(z_j), \\
 &\dots
 \end{aligned}$$

By using the ANOVA expansion we can represent both the parametric dependence as well as the dependence on phase variables in the solution to a kinetic equation. In the first case, the ANOVA approach can be readily applied to the probabilistic collocation method with appropriate anchor points [64,54,68,52,62], where we take the anchor points as the mean value of the random variable in each direction. Then, the PDF equations in Table 1 can be solved at the reduced number of collocation points in the parametric space according to the ANOVA decomposition. On the other hand, representing the dependence of the solution PDF on the phase variables through the ANOVA expansion yields a hierarchy of coupled PDF equations that resembles the BBGKY closures we presented in section 2.2. However, we comment that the BBGKY closure is more convenient than the ANOVA approach due to its less intrusive derivation.

3. Computational cost

Let us consider a kinetic partial differential equation with n phase variables and m parameters, i.e., a total number of $N = n + m$ variables. Suppose that we represent the solution by using q_z degrees of freedom⁵ in each phase variable and q_b degrees of freedom in each parameter. Thus, by using a regular tensor product, the number of degrees-of-freedom becomes $q_z^n q_b^m$ and the computational cost grows exponentially as $O(q_z^{2n} q_b^m)$. If we consider the sparse grid collocation for the parametric space, the cost reduces to a logarithmic growth in m , but still suffers from the curse of dimensionality. Hereafter, we compare the computational cost of the methods we discussed in the previous sections that reveal less computational complexity.

ANOVA series expansion and BBGKY closures

If we consider the ANOVA expansion or the BBGKY hierarchy, the computational complexity has a factorial dependence on the dimensionality $n + m$ and the interaction orders of the variables v . In particular, the number of degrees-of-freedom assuming that $q_b = q_z$ becomes $\sum_{s=1}^v C(n + m, s, q_z)$, where

$$C(N, s, q_z) \stackrel{\text{def}}{=} q_z^s \binom{N}{s}. \tag{24}$$

Regarding the matrix–vector operations for the discretized variables in each level, the computational cost follows as $O(C(n + m, v, q_z^{2v}))$. Let us describe the cost in detail by considering the phase space and the parameter space separately. When high-dimensionality only appears in the parameter space, the probabilistic collocation ANOVA method can be combined with the tensor product in the phase space. In that case, the degree of freedom and the computational cost becomes $q_z^n \sum_{s=1}^v C(m, s, q_b)$ and $O(q_z^{2n} C(m, v, q_b^v))$. On the other hand, if the phase space is in high-dimension, the application of the BBGKY closure will reduce the computational cost to $O(C(n, v, q_z^v) q_b^m)$. Finally, we remark that instead of considering the BBGKY closure in the entire space, it is reasonable to combine it with the ANOVA approach for further accuracy, since the interaction order of the phase variables and the parameters, denoted as v and v' , can be controlled separately. In this case, the number of degrees-of-freedom and the computational cost becomes $(\sum_{s=1}^v C(n, s, q_z)) (\sum_{s=1}^{v'} C(m, s, q_b))$ and $O(C(n, v, q_z^v) C(m, v', q_b^{v'}))$. The computational costs of these methods are summarized in Table 2.

Separated series expansion (SSE)

The total number of degree of freedoms in the SSE method is $Rnq_z + Rmq_b$, i.e., it grows linearly with both n and m (see Table 2). In particular, if the separation rank R is relatively small then the separated expansion method is much more efficient than tensor product, sparse grid or ANOVA approaches, both in terms of memory requirements as well as in terms of computational cost. The alternating-direction algorithm at the basis of the separated series expansion method can be divided into two steps, i.e., the enrichment and the projection steps (see Table 3). For a separation rank r , the number of operations to perform these steps is $O(rq_z^2 + (rq_z)^3)$. Since we begin from the first basis vector and gradually increase the separation rank, this cost has to be summed up to $r = 1, \dots, R$, and finally multiplied by the average number of iterations n_{itr} required to achieve the target accuracy ϵ . The computational cost of the projection step can be neglected with respect

⁵ In a spectral collocation setting, q_z is the number of collocation points in each phase variable.

Table 2

Number of degrees-of-freedom and computational cost of solving kinetic equations by using different methods. Shown are results for ANOVA method, BBGKY closures, and Separated Series Expansion (SSE). In the table, n and m denote the number of phase variables and parameters appearing in the kinetic equation, respectively. We are assuming that we are representing the PDF solution with q_z degrees of freedom in each phase variable and q_b in each parameter. Also, R is the separation rank and n_{iter} is the average number of iterations required for convergence of the separated expansion. The quantity ν is the interaction order of the ANOVA expansion or the BBGKY closure in the PDF solution.

	Degrees of freedom	Computational Cost
ANOVA	$q_z^n \sum_{s=1}^{\nu} q_b^s \binom{m}{s}$	$O(q_z^{2n} q_b^{2\nu} \binom{m}{\nu})$
BBGKY	$\sum_{s=1}^{\nu} q_z^s \binom{n+m}{s}$	$O(q_z^{2\nu} \binom{n+m}{\nu})$
SSE	$R n q_z + R m q_b$	$O(R^4 n q_z^3 + R^4 m q_b^3) n_{itr}$

to the one of the enrichment step, as it reduces to solving a linear system of rather small size ($R \times R$). Thus, the overall computational cost of the separated expansion method can be estimated as $O(R^4 n q_z^3 + R^4 m q_b^3) n_{itr}$, and it can be reduced to $O(R^3 n q_z^2 + R^3 m q_b^2) n_{itr}$ by using appropriate iterative linear solvers.

4. Numerical results

In this section we provide numerical examples to demonstrate the effectiveness of the numerical methods we proposed in the paper. To this end, we will consider kinetic partial differential equations corresponding to stochastic PDEs as well as stochastic dynamical systems.

4.1. Stochastic advection of scalar fields

We consider the following two stochastic advection equations

$$\frac{\partial u}{\partial t} + \left(1 + \sum_{k=1}^m \frac{1}{2k} \sin(kt) \xi_k(\omega) \right) \frac{\partial u}{\partial x} = 0, \tag{25}$$

$$\frac{\partial u}{\partial t} + \frac{\partial u}{\partial x} = \sin(t) \sum_{k=1}^m \frac{1}{5(k+1)} \sin((k+1)x) \xi_k(\omega), \tag{26}$$

where $x \in [0, 2\pi]$ and $\{\xi_1, \dots, \xi_m\}$ are i.i.d. uniform random variables in $[-1, 1]$. As we have shown in [17], the kinetic equations governing the joint probability density function of $\{\xi_1, \dots, \xi_m\}$ and the solution to (25) or (26) are, respectively,

$$\frac{\partial p}{\partial t} + \left(1 + \sum_{k=1}^m \frac{1}{2k} \sin(kt) b_k \right) \frac{\partial p}{\partial x} = 0, \tag{27}$$

$$\frac{\partial p}{\partial t} + \frac{\partial p}{\partial x} = - \left(\sin(t) \sum_{k=1}^m \frac{1}{5(k+1)} \sin((k+1)x) b_k \right) \frac{\partial p}{\partial z}, \tag{28}$$

where $p = p(x, t, z, \mathbf{b})$, $\mathbf{b} = \{b_1, \dots, b_m\}$. Note that this PDF depends on x, t , one phase variable z (corresponding to $u(x, t)$) and m parameters \mathbf{b} (corresponding to $\{\xi_1, \dots, \xi_m\}$). The analytical solutions to Eqs. (27) and (28) can be obtained by using the method of characteristics [69]. They are both in the form

$$p(x, t, z, \mathbf{b}) = p_0(x - X(t, \mathbf{b}), z - Z(x, t, \mathbf{b}), \mathbf{b}), \tag{29}$$

where $p_0(x, z, \mathbf{b})$ is the initial joint PDF of $u(x, t_0)$ and $\{\xi_1, \dots, \xi_m\}$, and

$$X(t, \mathbf{b}) = t - \sum_{k=1}^m \frac{(\cos(kt) - 1) b_k}{2k^2}, \quad Z(x, t, \mathbf{b}) = 0$$

in the case of equation (27), and

$$X(t, \mathbf{b}) = t, \quad Z(x, t, \mathbf{b}) = \sum_{k=2}^{m+1} \frac{b_{k-1}}{10k} \left(\frac{\sin(kx - t)}{k-1} - \frac{\sin(kx + t)}{k+1} - \frac{2 \sin(k(x-t))}{(k-1)(k+1)} \right)$$

in the case of equation (28). In particular, in our simulations we set

$$p_0(x, z, \mathbf{b}) = \left(\frac{\sin^2(x)}{2\pi\sigma_1} \exp\left[-\frac{(z - \mu_1)^2}{2\sigma_1}\right] + \frac{\cos^2(x)}{2\pi\sigma_2} \exp\left[-\frac{(z - \mu_2)^2}{2\sigma_2}\right] \right) \exp\left[-\frac{|\mathbf{b}|^2}{2}\right],$$

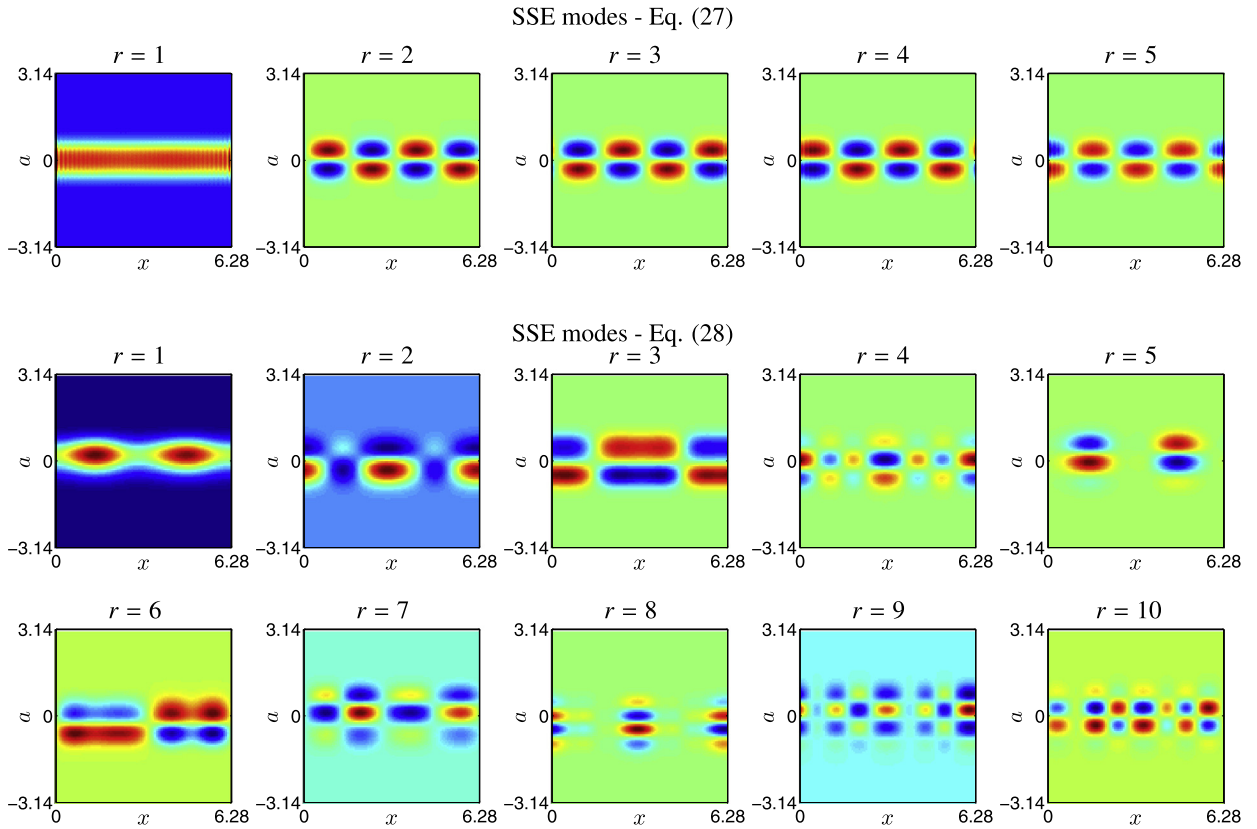


Fig. 4. Stochastic advection problem: separated series expansion modes on the physical and response space, that is, $p_x^r(x)p_z^r(z)$ at $t = 2$. (For interpretation of the colors in this figure, the reader is referred to the web version of this article.)

which has separation rank $R = 2$. Non-separable initial conditions can be approximated in terms of series expansions in the form (1). We consider high-dimensional parametric space for $m = 3, 13, 24, 54, 84, 114$ and compare the SSE algorithm and the ANOVA decomposition that work efficiently for this type of problems.

We computed the solution to (27) and (28) by using a separated series expansion and the ANOVA expansion. The alternating-direction Galerkin method proposed in section 2.1 computes the solution in the form

$$p(x, t, z, \mathbf{b}) \simeq \sum_r \alpha_r(t) p_x^r(x) p_z^r(z) p_1^r(b_1) \cdots p_m^r(b_m), \tag{30}$$

where the dependence on x and z is represented by using a Fourier spectral collocation method with $q_z = 50$ degrees of freedom in each variable, while the parametric dependence on b_k ($k = 1, \dots, m$) is represented with probabilistic collocation method based on the Legendre polynomials of order⁶ $q_b = 7$. On the other hand, the solution considering the ANOVA expansion in the excitation space is in the form

$$p(x, t, z, \mathbf{b}) \simeq q_0(x, z) + \sum_{i=1}^m q_i(x, z) q_i^b(b_i) + \sum_{i < j}^m q_{ij}(x, z) q_{ij}^b(b_i, b_j) + \cdots. \tag{31}$$

The solutions (30) and (31) are computed at each time step ($\Delta t = 10^{-2}$) up to $t = 3$ by using the Crank–Nicolson scheme (4) and the second-order Runge–Kutta, respectively.

In Fig. 4, we plot the first few modes $p_x^r(x)p_z^r(z)$ of the separated series solution to Eqs. (27) and (28) with $m = 54$ and $m = 3$, respectively. In the case of Eq. (27), $p_x^r(x)p_z^r(z)$ look very similar to each other for $r \geq 2$, while in the case of Eq. (28) they are all different, suggesting the presence of modal interactions and a larger separation rank to achieve a prescribed target accuracy. This is also seen in Fig. 5, where we plot the normalization coefficients $\{\alpha_1, \dots, \alpha_R\}$. Since α_r can be interpreted as the spectrum of the separated PDF solution, we see that the stochastic advection problem (26) yields a stronger coupling between the modes, i.e., a slower spectral decay than the problem (25).

⁶ The number of degrees-of-freedom of the discretized space should be chosen carefully to balance the errors between the space and time discretization and the truncation of the separated series. By considering $q_b = 7$ in this example, the error is dominated by the truncation of the separation rank.

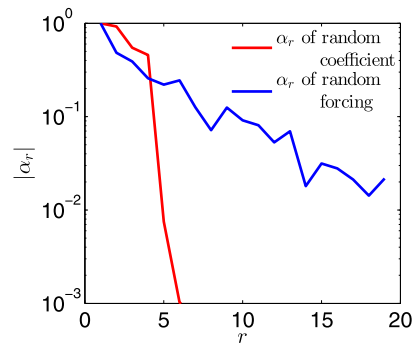


Fig. 5. Stochastic advection problem: spectra of the separated series expansion at $t = 2$.

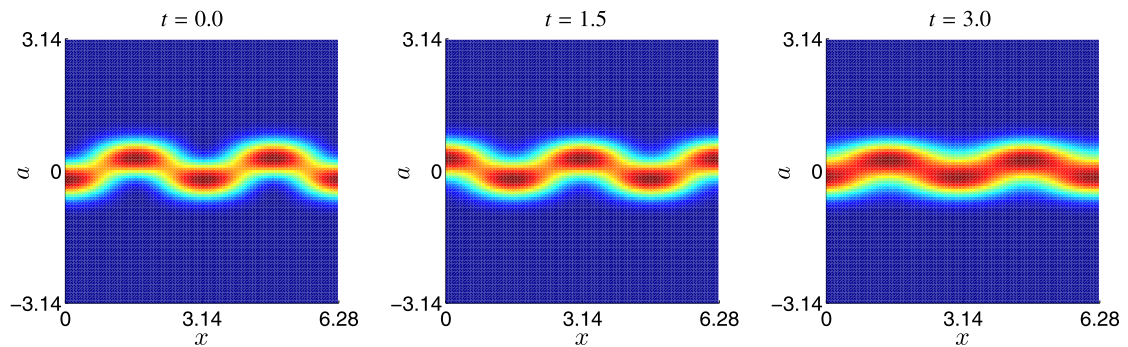


Fig. 6. Stochastic advection problem (25): PDF of the solution at different times. The PDF dynamics is obtained by solving (27) with a separated series expansion. The separation rank is set to $R = 8$, and we consider $m = 54$ random variables in (25). (For interpretation of the colors in this figure, the reader is referred to the web version of this article.)

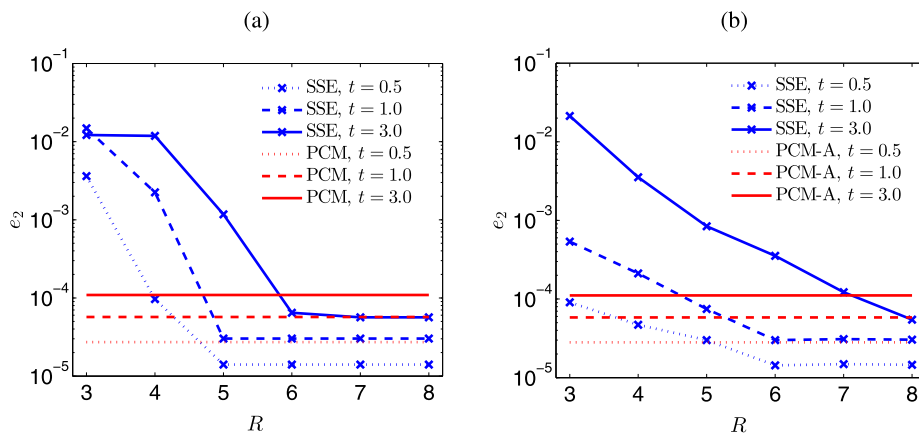


Fig. 7. Stochastic advection problem (25): relative L_2 errors of using the full tensor product (PCM), the separated series expansion (SSE), and the ANOVA approach (PCM-A, level 2) with respect to the analytical solution (29). Shown are results at $t = 0.5$, $t = 1$ and $t = 3$ for different separation ranks R and different number of random variables: $m = 3$ (a) and $m = 54$ (b).

In Fig. 6, we plot the PDF of the solution to Eq. (25). Such a PDF is obtained by first solving (27) by using the separated expansion method, and then integrating (30) numerically with respect to $\{b_1, \dots, b_m\}$. Convergence with respect to R is demonstrated in Fig. 7. Note that the separated expansion method reaches the same error level as the ANOVA approximation with just five modes for $t \leq 1$, but it requires a larger separation rank at later times in order to keep the same accuracy. In addition, the convergence rate of the separated expansion method saturates with R due to time integration errors. In Fig. 8, we show the PDF of the solution to the advection problem (26) at different times, where we have considered a random forcing term with $m = 24$ random variables. Such a PDF is obtained by solving (28) with a separated series expansion (30) of rank $R = 8$. Convergence with respect to R is demonstrated in Fig. 9. It is seen that the convergence rate in this case is slower than in the previous example (see Fig. 7), and the overall relative error is larger. This is due to the presence of the time-dependent forcing term in Eq. (26), which injects additional energy in the system and yields new SSE modes

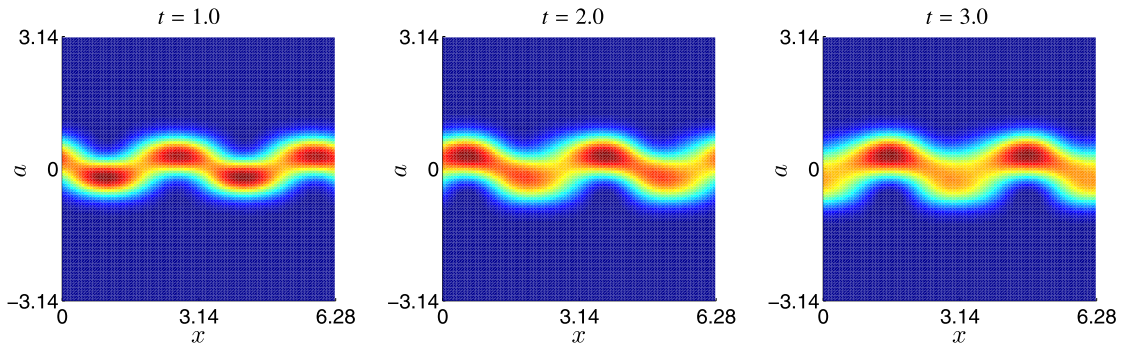


Fig. 8. Stochastic advection problem (26): PDF of the solution at different times. The PDF dynamics is obtained by solving (28) with a separated series expansion. The separation rank is set to $R = 8$, and we consider $m = 24$ random variables in (26). (For interpretation of the colors in this figure, the reader is referred to the web version of this article.)

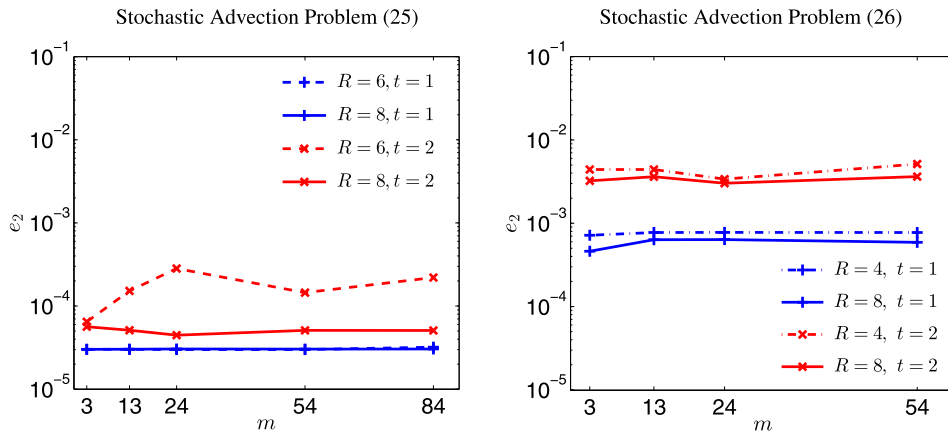


Fig. 9. Stochastic advection problem: relative L_2 errors of the separated PDF solutions with respect to the analytical solution (29). Shown are results for different number of random variables m in (25)–(26) and different separation ranks R . It is seen that the accuracy of the separated expansion method mainly depends on the separation rank rather than on the number of random variables.

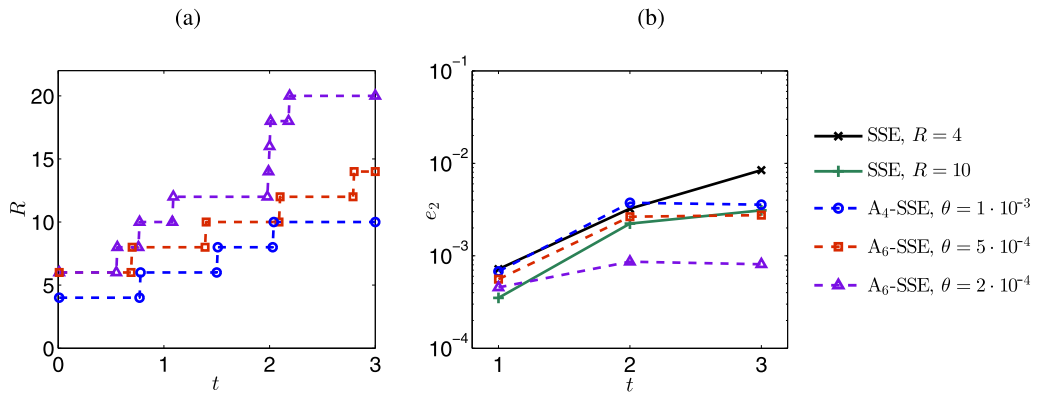


Fig. 10. Adaptive SSE algorithm: separation rank R (a) and relative L_2 error (b) versus time for different thresholds θ initiated with a separation rank r (A_r -SSE). A small θ yields a large separation rank and a small relative error.

(see Fig. 4). This yields a higher separation rank for a prescribed level of accuracy. In addition, the plots suggest that the accuracy of the separated expansion method depends primarily on the separation rank R of the solution rather than on the dimensionality of the random forcing vector.

So far, we fixed the separation rank R throughout our simulations, to investigate convergence and accuracy of the separated series expansion method. However, in practical applications, the appropriate separation rank should be identified on-the-fly, i.e., while the simulation is running. To address this question, in the previous section, we propose an adaptive strategy based on the spectrum $\alpha = \{\alpha_1, \dots, \alpha_R\}$ of the separated series, that is, increasing the separation rank R if the ratio

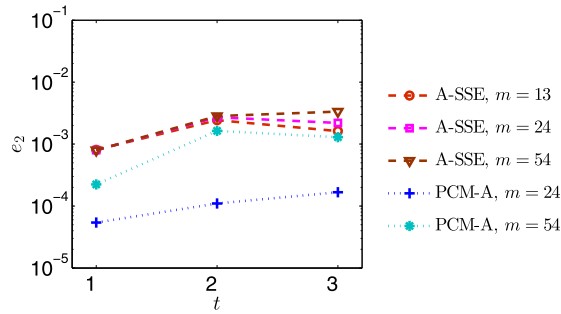


Fig. 11. Adaptive SSE algorithm: comparison between the relative L_2 errors of the adaptive separated expansion method (A-SSE) and the ANOVA (PCM-A, level 2) method. Results are for the kinetic equation (28) with threshold $\theta = 5 \cdot 10^{-4}$. It is seen that the error of the A-SSE method is slightly independent of m , while the error of ANOVA level 2 increases as we increase m .

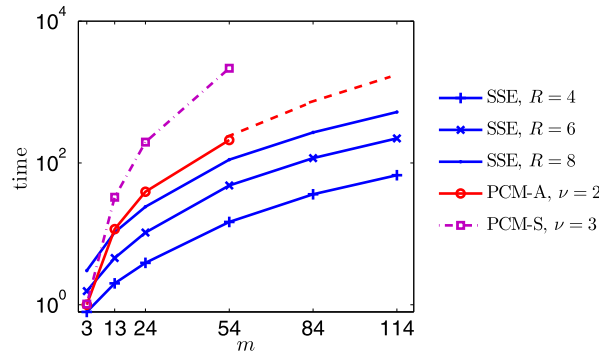


Fig. 12. Computational time (in seconds) of the separated expansion method (SSE), and probabilistic collocation ANOVA level 2 (PCM-A) and sparse grid level 3 (PCM-S) as a function of the number of random variables m and separation rank R . The results are normalized with respect to the computing time of using the tensor product with $m = 3$. The dotted lines correspond to extrapolations based on short-runs estimates.

$\alpha_R/\alpha_1 > \theta$. The corresponding adaptive algorithm initialized with a separation rank r is denoted as A_r -SSE, and it is studied hereafter with reference to Eq. (28). In Fig. 10 we plot R versus time for different thresholds θ . It is seen that the adaptive algorithm yields a separation rank that increases in time. In particular, the case $\theta = 10^{-3}$ yields $R = 10$ at $t = 3$, which results in a slightly larger error than the one obtained for fixed $R = 10$. In Fig. 11, we compare the accuracy of the A_6 -SSE method with $\theta = 5 \cdot 10^{-4}$ and the ANOVA method (level 2). Specifically, we study the relative L_2 error of the solution to Eq. (28) for different number of random variables, i.e., $m = 13$, $m = 24$, and $m = 54$. We first notice that the error in the A_6 -SSE method seems to be slightly independent of m . On the other hand, the error of ANOVA method increases with m , although such an error can be improved by increasing the interaction order. However, this would yield an increasing number of collocation points. For example, increasing the interaction order from two to three for $m = 54$ would increase the number of collocation points from 70 498 to 8 578 270 (see [64]). In Fig. 12, we compare the computational time of the separated series expansion method, with the ANOVA method of level two and sparse grid of level three on the excitation space. The simulations are performed on a single CPU of Intel Xeon E5540 (2.53 GHz) and the results are normalized with respect to the computing time using the tensor product for the case $m = 3$. It is seen that the separated expansion method costs less than the ANOVA level 2 when $m \geq 24$ and $R \leq 8$. In the case of equation (27), the separated expansion method is more efficient than ANOVA, as it reaches the same error level with a small separation rank ($R < 8$).

In summary, the separated series expansion method is effective for high-dimensional kinetic equations provided the solution has a small separation rank. If the separation rank is relatively large, then the ANOVA method is expected to be more efficient, although a rigorous quantification of this statement should be done on a case-by-case basis.

4.2. Lorenz-96 system

The Lorenz-96 system is a continuous in time and discrete in space model often used in atmospheric sciences to study fundamental issues related to forecasting and data assimilation [70,71]. The basic equations are

$$\frac{dx_i}{dt} = (x_{i+1} - x_{i-2})x_{i-1} - x_i + F, \quad i = 1, \dots, n. \tag{32}$$

Here we consider $n = 40$, $F = 1$, and assume that the initial state $\mathbf{x}(0) = [x_1(0), \dots, x_{40}(0)]$ is jointly Gaussian with PDF

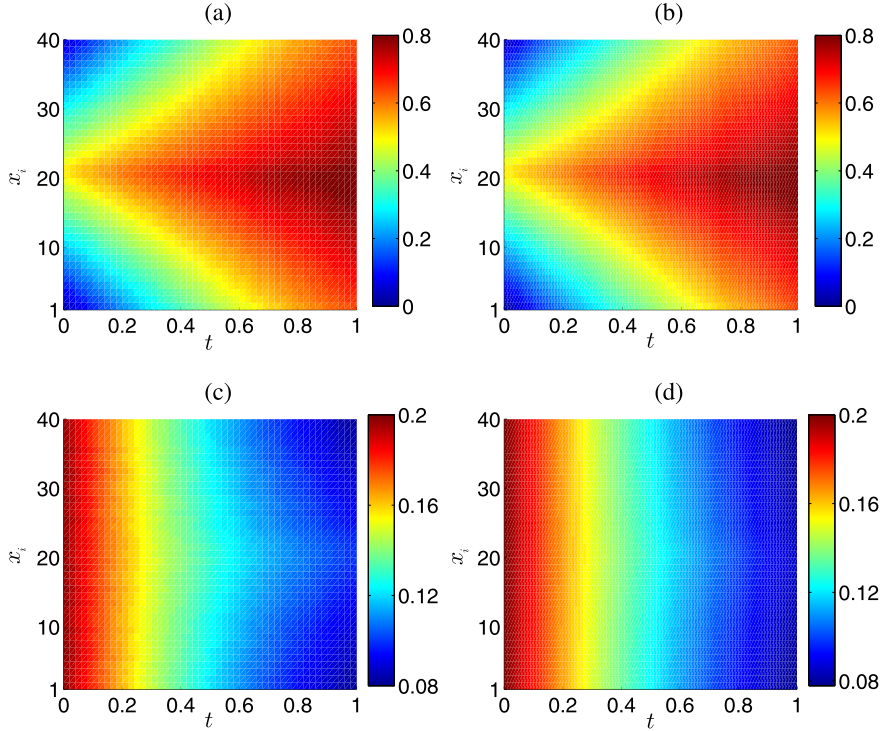


Fig. 13. Lorenz-96 system: The mean (a), (b) and standard deviation (c), (d) computed by the one-point (a) two-points (c) BBGKY closure compared to the Monte-Carlo simulation (b), (d). (For interpretation of the colors in this figure, the reader is referred to the web version of this article.)

$$p(z_1, \dots, z_{40}, t = 0) = \left(\frac{25}{2\pi}\right)^{20} \prod_{i=1}^{40} \exp\left[-\frac{25}{2}\left(z_i - \frac{i}{40}\right)^2\right]. \quad (33)$$

Thus, in this system we have $n = 40$ phase variables and $m = 0$ parameters, i.e., $N = n$. The kinetic equation governing the joint PDF of the phase variables $\mathbf{x}(t) = [x_1(t), \dots, x_{40}(t)]$ is

$$\frac{\partial p(\mathbf{z}, t)}{\partial t} = -\sum_{i=1}^{40} \frac{\partial}{\partial z_i} [(z_{i+1} - z_{i-2})z_{i-1} - z_i + F] p(\mathbf{z}, t), \quad \mathbf{z} \in \mathbb{R}^{40} \quad (34)$$

and it cannot be obviously solved in a tensor product representation because of high-dimensionality and possible lack of regularity (for $F > 10$) related to the fractal structure of the attractor [71]. Thus, we are led to look for reduced-order PDF equations. Specifically, we consider here the one-point and two-points BBGKY closures we discussed in section 2.2. The first one yields the approximated system

$$\frac{\partial p_i(z_i, t)}{\partial t} = -\frac{\partial}{\partial z_i} [(\langle x_{i+1} \rangle - \langle x_{i-2} \rangle) \langle x_{i-1} \rangle_{i-1|i} - (z_i - F) p_i(z_i, t)], \quad (35)$$

where $\langle \cdot \rangle_{i|j}$ is defined in (21). In order to close such a system within the level of one-point PDFs, $\langle x_{i-1} \rangle_{i-1|i}$ could be replaced, e.g., by $\langle x_{i-1} \rangle p(z_i, t)$. Similarly, the two-points BBGKY closure of the adjacent nodes yields the hierarchy

$$\begin{aligned} \frac{\partial p_{i+1}(z_i, z_{i+1}, t)}{\partial t} = & -\frac{\partial}{\partial z_i} [z_{i+1} \langle x_{i-1} \rangle_{i-1|i} p_{i+1}(z_i, t) - \langle x_{i-2} \rangle \langle x_{i-1} \rangle_{i-1|i} p_{i+1}(z_i, t) \\ & - (z_i - F) p_{i+1}(z_i, z_{i+1}, t)] - \frac{\partial}{\partial z_{i+1}} [\langle x_{i+2} \rangle_{i+2|i+1} z_i p_i(z_i, t) - \langle x_{i-1} \rangle z_i p_{i+1}(z_i, z_{i+1}, t) \\ & - (z_{i+1} - F) p_{i+1}(z_i, z_{i+1}, t)]. \end{aligned} \quad (36)$$

By adding the two-points closure of one node apart, i.e., x_{i-1} and x_{i+1} , the quantity $\langle x_{i-2} \rangle \langle x_{i-1} \rangle_{i-1|i} p_{i+1}(z_i, t)$ in the first row and $\langle x_{i-1} \rangle z_i p_{i+1}(z_i, z_{i+1}, t)$ in the second row can be substituted by $\langle x_{i-2} \rangle_{i-2|i} \langle x_{i-1} \rangle_{i-1|i+1}$ and $\langle x_{i-1} \rangle_{i-1|i+1} z_i p_i(z_i, t)$, respectively. In our simulation, we alternate between the two approximations at every time step. Each equation in (35)–(36) is discretized by using a Fourier spectral collocation method with $q_z = 64$ degrees of freedom in each variable, and fourth-order Runge–Kutta time integration with $\Delta t = 10^{-3}$.

In Fig. 13, we plot the mean and the standard deviation of the solution to (32) computed by the one- and two-points BBGKY closures and the Monte Carlo simulation – 50 000 solution samples. It is seen that the mean of the BBGKY closure

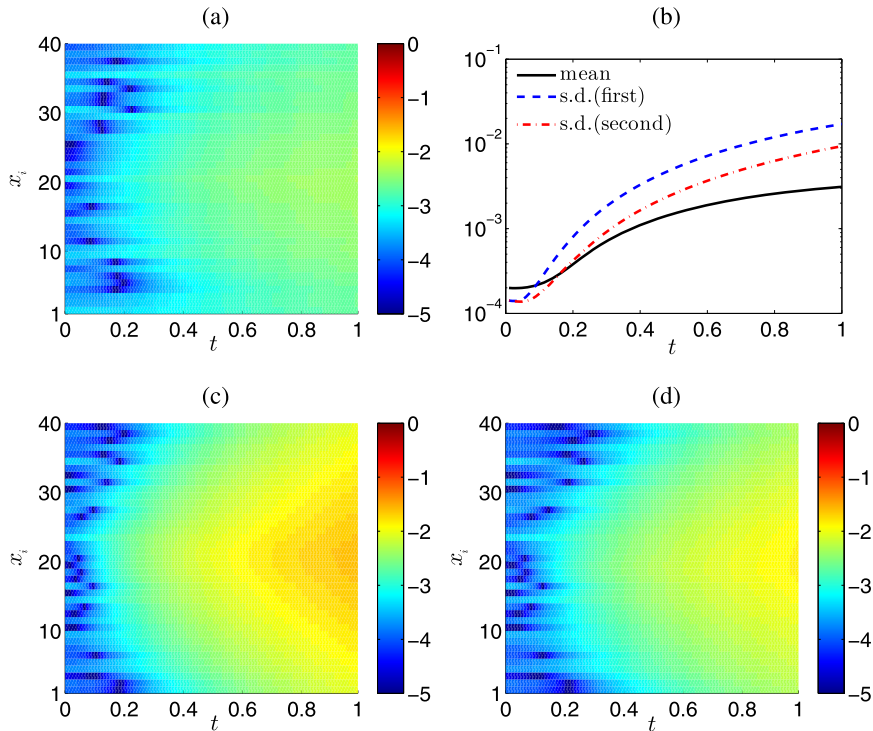


Fig. 14. Lorenz-96 system: The absolute error of the mean (a) and standard deviation (c), (d) by using the BBGKY closure compared to the Monte-Carlo simulation in log-scale. In (c) and (d), the results are computed by the one- and two-points BBGKY closure (Eqs. (35) and (36), respectively) and the L_1 error is shown in (b). (For interpretation of the colors in this figure, the reader is referred to the web version of this article.)

coincides with the one obtained from the Monte Carlo and the one-point closure. However, the standard deviation is slightly different. The absolute error in log-scale compared to the Monte Carlo simulation is shown in Fig. 14, where we observe the reduced error in the standard deviation by involving the two-points PDFs. This can be also seen in Fig. 14(b) where we plot the L_1 error of the moments. Note that adding the two-points PDFs to the hierarchy in this case improves the error in the standard deviation by a small amount.

4.3. Stochastic diffusion equation

An interesting question arises whether it is possible to determine a closed PDF evolution equation of the solution to second order PDEs at a specific space–time location. Unfortunately, the answer is negative due to its nonlocal solutions in space and time. This nonlocal feature yields the impossibility to determine a point-wise equation for the probability density. Still, there has been extensive studies to tackle this problem by use of functional integral methods, in particular those involving the Hopf characteristic functional [72–74]. Here we consider the semi-discrete form of PDEs that can be written in a form of multi-dimensional dynamical system that yields a Liouville type PDF equation. Afterwards, the BBGKY closure is employed to the corresponding multi-dimensional PDF system, combined with the ANOVA method in case we have a high-dimensional excitation space.

Let us consider a diffusion equation as follows:

$$\frac{\partial u}{\partial t} = \frac{\partial}{\partial x} \left(\mu(x, t; \omega) \frac{\partial u}{\partial x} \right), \quad (37)$$

where $x \in [0, 2\pi]$, $t \geq 0$ and $\mu(x, t; \omega) > 0$ is the random diffusivity. This equation is accompanied by a periodic boundary condition $u(0, t; \omega) = u(2\pi, t; \omega)$ and $u_x(0, t; \omega) = u_x(2\pi, t; \omega)$. We then discretize the solution in the physical space by using a set of orthogonal basis functions in $L^2([0, 2\pi])$. Here, we consider the Fourier basis functions as

$$u(x, t; \omega) = \hat{u}_0(t; \omega) + \sum_k (\hat{u}_k(t; \omega) \sin(kx) + \hat{u}_{-k}(t; \omega) \cos(kx)). \quad (38)$$

We assume that we have available a similar representation for the diffusivity $\mu(x, t; \omega)$ with coefficients $\{\hat{\mu}_k(t; \omega)\}$ in terms of random variables as $\hat{\mu}_k(t; \omega) = \hat{\mu}_k(t; \xi(\omega))$. Then, the dimensionality of the kinetic equation depends on the truncation of the solution (38) and the parameters. In other words, the dimensionality can be as high as the number of basis functions, which will be necessary when the solution in the physical space has low regularity. Thus, we employ the BBGKY closure

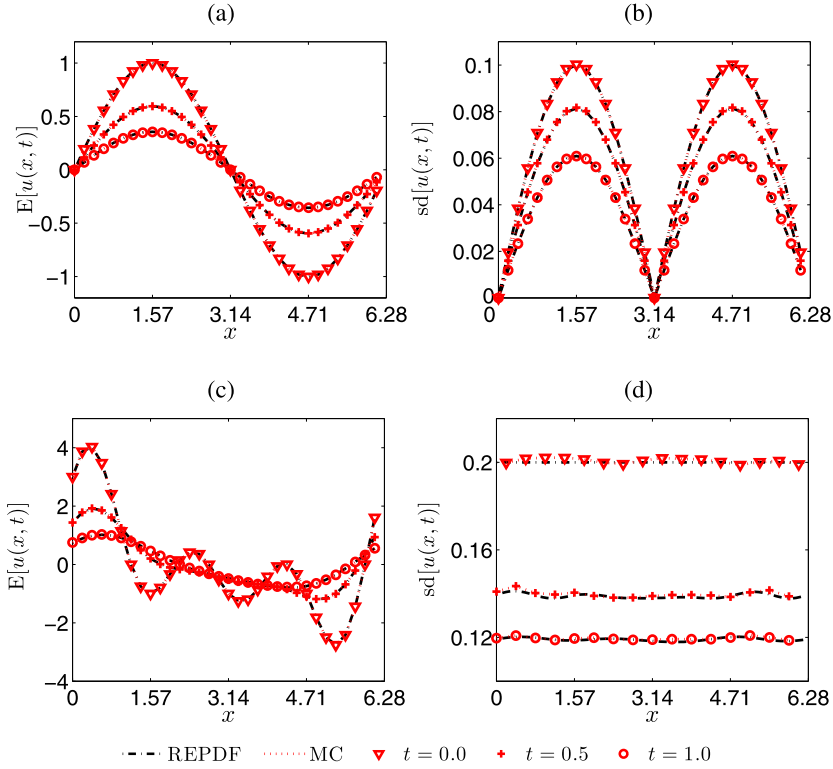


Fig. 15. The mean (a), (c) and standard deviation (b), (d) of the solution to the heat equation with time-correlated random coefficient with correlation length $l_c = 0.1$ (a), (b) and space dependent coefficient (c), (d) up to time $t = 1$. The shown results are computed by the PDF (REPDF) and the Monte Carlo (MC) approach, where we cannot visually distinguish the difference in the results.

approach developed in Section 2.2 to obtain a reduced-order PDF equation, approximating the system within lower order interactions. When the random coefficient is independent of the physical variable, the Fourier modes are independent. Therefore, we can truncate the BBGKY closure at the level of one-point PDFs. The equation becomes

$$\frac{\partial p_k(z_k, t)}{\partial t} = -\frac{\partial}{\partial z_k} \left[-k^2 \mu(t, b_\mu) z_k p_k(z_k) \right], \tag{39}$$

where b_μ is a vector of parametric random variables. In case of space dependent coefficients, interactions between the Fourier coefficients occur. Hence, it becomes inevitable to include the higher-order joint PDFs. We compute the two-point BBGKY closure for the joint PDF equation of the k -th and l -th coefficient as

$$\frac{\partial p_{kl}(z_k, z_l, t)}{\partial t} = -\frac{\partial}{\partial z_k} [\mathbb{Q}(p_{kl}, k)] - \frac{\partial}{\partial z_l} [\mathbb{Q}(p_{kl}, l)], \tag{40}$$

where

$$\mathbb{Q}(p_{ij}, i) \stackrel{\text{def}}{=} \begin{cases} -i^2 \hat{\mu}_0 z_i p_{ij} + \sum_{n+m=i} \left(\frac{mi}{2} (-\hat{\mu}_n \langle z_{-m} \rangle_{-m|i} - \hat{\mu}_{-n} \langle z_m \rangle_{m|i}) \right) p_j \\ \quad + \sum_{n-m=|j|} \left(\frac{m(n-m)}{2} (\hat{\mu}_n \langle z_{-m} \rangle_{-m|i} - \hat{\mu}_{-n} \langle z_m \rangle_{m|i}) \right) p_j, & i \geq 0 \\ -i^2 \hat{\mu}_0 z_i p_{ij} + \sum_{n+m=|j|} \left(-\frac{mi}{2} (\hat{\mu}_n \langle z_m \rangle_{m|i} - \hat{\mu}_{-n} \langle z_{-m} \rangle_{-m|i}) \right) p_j \\ \quad + \sum_{n-m=|j|} \left(\frac{m(n-m)}{2} (\hat{\mu}_n \langle z_m \rangle_{m|i} + \hat{\mu}_{-n} \langle z_{-m} \rangle_{-m|i}) \right) p_j, & i < 0. \end{cases} \tag{41}$$

Here, $\langle \cdot \rangle_{m|i}$ is defined as in Eq. (21), and the arguments of $\hat{\mu}_n$ are omitted. Finally, when the dimensionality of the parametric space exceeds three, we employ the ANOVA decomposition.

We first consider a time-dependent random coefficient for the diffusion term, and compute the solution by using the one-point BBGKY closure (39). In particular, we take a log-normal random coefficient $\mu(t; \omega)$ defined as $V(t; \omega) = \log(\mu(t; \omega))$, where $V(t; \omega)$ is a mean-zero exponentially correlated Gaussian process with correlation time $l_c = 0.1$. The coefficient is represented by using the Karhunen–Loève expansion in a series expansion form. It involves 20 Gaussian random variables, that is truncated to achieve 97% of the eigen-spectrum, and we employ the ANOVA method of level two for the collocation basis based on the Hermite polynomials. We simply consider the initial solution $u(x, t = 0; \omega) = \sin(x)\eta_1(\omega)$ with a Gaussian random variable $\eta_1(\omega) = N(1, 0.1)$, which makes the initial condition of the BBGKY closure as $p_{\eta_1}(z_1)$. Thus, the

total dimensionality of the kinetic equation is 21. For the time integration, we employ the fourth-order Runge–Kutta method with time step $\Delta t = 10^{-3}$. Fig. 15 shows the evolution of the mean and standard deviation of the solution at time $t = 0, 0.5, 1$. The BBGKY results coincide with the reference solution computed by using the Monte-Carlo simulation with 50,000 samples, and we remark that the relative L_2 error stays at the level of $O(10^{-4})$.

In case of a space dependent random coefficient, we consider $V(x; \omega) = \log(2\mu(x; \omega))$, where $V(x; \omega) = \sum_{k=1}^2 (\sin(kx)\xi_k(\omega) + \cos(kx)\xi_{-k}(\omega))$ and $\xi_k(\omega) \sim N(0, 1/3^2)$ for all k 's. Here, we compute the PDF by using the two-points closure (40). By taking the initial solution as $u(x, t = 0; \omega) = \eta_0(\omega) + \sum_{k=1}^3 (\sin(kx)\eta_k(\omega) + \cos(kx)\eta_{-k}(\omega))$, with independent Gaussian random variables $\eta_k(\omega) = N(1, 0.1)$ for $k \neq 0$ and $\eta_0(\omega) = N(0, 0.1)$, the initial condition for the two-points BBGKY closure becomes $p_{kl}(z_k, z_l, t = 0) = p_{\eta_k}(z_k)p_{\eta_l}(z_l)$. We take the resolution of the solution to be the same as the initial condition by using seven Fourier coefficients. Thus, the kinetic equation lies in an 11-dimensional space with seven phase variables and four parameters. Again, the parametric space is accompanied with the ANOVA method of level two. Fig. 15 compares the mean and standard deviation compared to 50,000 Monte Carlo simulations at time $t = 0, 0.5, 1$, and the two lines cannot be visually distinguished. For both of the first and second moment, the relative L_2 error stays within the level of $O(10^{-3})$. Thus, we conclude that the PDF of the solution to a time and space dependent diffusion equation can be computed with reasonable accuracy considering the time step and the truncation of the computational domain by using the BBGKY closures and ANOVA approach.

5. Summary and discussion

In this paper we proposed and validated three different classes of new algorithms to compute the numerical solution of high-dimensional kinetic partial differential equations. The first class of algorithms is based on separated series expansions (SSE) and it yields a sequence of low-dimensional problems that can be solved recursively and in parallel by using alternating direction methods. In particular, we developed a new algorithm that updates the entire rank of the separated representation in each variable, minimizing separation rank and improving the convergence rate. We also proposed an adaptive version of such an algorithm and we demonstrated its effectiveness in numerical applications to random advection of passive scalar fields. The second class of algorithms we proposed is based on a hierarchy of coupled probability density function equations that resembles the BBGKY [50] and the Lundgren–Monin–Novikov [75,76] hierarchies. We studied the accuracy and the computational efficiency of low-order truncations of the hierarchy (BBGKY closure) for the Lorenz-96 system and the semi-discrete form of the diffusion equation. The third class of algorithms relies on high-dimensional model representations (ANOVA expansions) and probabilistic (sparse) collocation methods. A common feature of all these methods is that they allow us to reduce the problem of computing the solution to high-dimensional kinetic equations to a sequence of low-dimensional problems. The range of applicability of proposed new algorithms is sketched in Fig. 1 as a function of the number of phase variables n and the number of parameters m appearing in the kinetic equation. The SSE scales linearly and the ANOVA method scales factorially with the dimension of the phase space, and they yield comparable results for moderate separation ranks. However, for large separation ranks the ANOVA method is preferable to SSE in terms of computational cost. We emphasize that the choice between ANOVA and SSE does not depend on the number of variables in the kinetic equation but rather on the properties of its solution, in particular the separation rank. In addition, in order to approximate the kinetic system regarding the interaction order between the variables, the BBGKY closure and the ANOVA method is convenient to be employed for the phase variable and the parameters, respectively.

Further developments of the proposed algorithms can be addressed along different directions. For example, one can consider tensor interpolative [77,78] and tensor train decompositions [79] to further improve the SSE method, by accelerating the rank reduction process. This is very useful when solving systems with large separation rank, such as those arising from Eq. (28). In addition, iterative solvers with appropriate preconditioners and adaptive methods can further reduce the computational cost of determining ANOVA and SSE decompositions (see [64] and section 2.1). Adaptive strategies can also be applied to the conditional moment approach by using variance-based sensitivity analysis, e.g., in terms of Sobol indices [60,61].

Acknowledgements

This work was supported by OSD-MURI Grant FA9550-09-1-0613, AFOSR Grant FA9550-14-1-0212 and NSF-DMS Grant 1216437.

Appendix A. Finite-dimensional representation of the alternating direction algorithm

In this appendix we provide additional details on the discretization of the alternating direction Galerkin algorithm proposed in section 2.1. To this end, let us first represent the basis functions appearing in joint probability density (1) in terms of polynomials as

$$p_n^r(z_n) = \sum_{j=1}^{q_z} p_{n,j}^r \phi_{n,j}(z_n), \quad (42)$$

where q_z is the number of degrees of freedom in each variable. For example, in section 4.1, we have considered a spectral collocation method in which $\{\phi_{1,j}\}$ and $\{\phi_{2,j}\}$ are trigonometric interpolants while $\{\phi_{n,j}\}_{n=3}^N$ are Lagrange interpolants through Gauss–Legendre–Lobatto points. The vector

$$\mathbf{p}_n^r = [\mathbf{p}_{n,1}^r, \dots, \mathbf{p}_{n,q_z}^r]$$

collects the (normalized) values of the solution at the collocation points. In such a collocation framework, we can write the expansion (1) in terms of a tensor product of degrees of freedom as

$$\mathbf{p} = \sum_{r=1}^{\infty} \alpha_r \mathbf{p}_1^r \otimes \dots \otimes \mathbf{p}_N^r. \tag{43}$$

Accordingly, the finite dimensional version of Eq. (12) is

$$\mathbf{A}\mathbf{p} = \mathbf{f},$$

where

$$\mathbf{A} = \sum_{k=1}^{n_A} \mathbf{A}_1^k \otimes \dots \otimes \mathbf{A}_N^k, \quad \mathbf{f} = \sum_{k=1}^{n_f} \mathbf{f}_1^k \otimes \dots \otimes \mathbf{f}_N^k, \tag{44}$$

$$\mathbf{A}_n^k[i, j] = \int \phi_{n,i}(z_n) A_n^k(z_n) \phi_{n,j}(z_n) dz_n, \quad \mathbf{f}_n^k[i] = \int f_n^k(z_n) \phi_{n,i}(z_n) dz_n. \tag{45}$$

By using a Gauss quadrature rule to evaluate the integrals, we obtain system matrices \mathbf{A}_n^k that either diagonal or coincide with the classical differentiation matrices of spectral collocation methods [80]. For example, in the case of equation (27) we have the components

$$\begin{aligned} \mathbf{A}_1^1[i, j] &= \mathbf{w}_x[i] \delta_{ij}, \quad \mathbf{A}_1^k[i, j] = \frac{\Delta t}{2} \mathbf{w}_x[i] \mathcal{D}_x[i, j], \quad k = 2, \dots, n_A, \\ \mathbf{A}_2^1[i, j] &= \mathbf{A}_2^2[i, j] = \mathbf{w}_z[i] \delta_{ij}, \quad \mathbf{A}_2^{k+2}[i, j] = \frac{\sin(kt_{n+1})}{2k} \mathbf{w}_z[i] \delta_{ij}, \quad k = 1, \dots, m, \\ \mathbf{A}_3^k[i, j] &= \mathbf{w}_b[i] \delta_{ij}, \quad k \neq 3, \quad \mathbf{A}_3^3[i, j] = \mathbf{w}_b[i] \mathbf{q}_b[i] \delta_{ij}, \quad \dots \end{aligned}$$

where \mathbf{q}_b denotes the vector of collocation points, \mathbf{w}_x , \mathbf{w}_z , and \mathbf{w}_b are collocation weights, \mathcal{D}_x is the differentiation matrix, and δ_{ij} is the Kronecker delta function. The alternating direction algorithm in the n -th direction yields a sequence of linear system

$$\mathbf{B}_n \widehat{\mathbf{p}}_n = \mathbf{b}_n, \tag{46}$$

where \mathbf{B}_n is a block matrix with $R \times R$ blocks of size $q_z \times q_z$, and \mathbf{b}_n is multi-component vector. Specifically, the h v -th block of \mathbf{B}_n and the h -th component of \mathbf{b}_n are obtained as

$$\mathbf{B}_n^{hv} = \sum_{k=1}^{n_A} \left(\prod_{i \neq n}^N [\mathbf{p}_i^h]^T \mathbf{A}_i^k \mathbf{p}_i^v \right) \mathbf{A}_n^k, \quad \mathbf{b}_n^h = \sum_{k=1}^{n_f} \left(\prod_{i \neq n}^N [\mathbf{p}_i^h]^T \mathbf{f}_i^k \right) \mathbf{f}_n^k.$$

The solution vector

$$\widehat{\mathbf{p}}_n = [\mathbf{p}_n^1, \dots, \mathbf{p}_n^R]^T$$

is normalized as $\mathbf{p}_n^r / \|\mathbf{p}_n^r\|$ for all $r = 1, \dots, R$ and $n = 1, \dots, N$. This operation yields the coefficients $\boldsymbol{\alpha} = (\alpha_1, \dots, \alpha_R)$ in (43) as a solution to the linear systems

$$\mathbf{D}\boldsymbol{\alpha} = \mathbf{d}, \tag{47}$$

where the entries of the matrix \mathbf{D} and the vector \mathbf{d} are, respectively

$$\mathbf{D}^{hv} = \sum_{k=1}^{n_A} \prod_{i=1}^N [\mathbf{p}_i^h]^T \mathbf{A}_i^k \mathbf{p}_i^v, \quad \mathbf{d}^h = \sum_{k=1}^{n_f} \prod_{i=1}^N [\mathbf{p}_i^h]^T \mathbf{f}_i^k.$$

The main steps of the algorithm are summarized in Table 3.

Stopping criterion. The stopping criterion for the alternating-direction algorithm is based on the condition $\|\mathbf{A}\mathbf{p}^R - \mathbf{f}\| < \varepsilon$, which involve the computation of an N -dimensional tensor norm. This can be quite expensive and compromise the com-

Table 3

Main steps of the proposed alternating-direction Galerkin algorithm.

```

Compute the separated representation of the initial condition  $\mathbf{p}(t_0)$ 
for  $t_1 \leq t_i \leq t_{n_f}$  do
  Compute  $\mathbf{f}$  by using  $\mathbf{p}(t_{i-1})$ 
  Set  $R = 1$ 
  while  $\|\mathbf{A}\mathbf{p}^R(t_i) - \mathbf{f}\| > \varepsilon$  do
    Initialize  $\{\tilde{\mathbf{p}}_1^R(t_i), \dots, \tilde{\mathbf{p}}_N^R(t_i)\}$  at random
    while  $\|\mathbf{A}\mathbf{p}^R(t_i) - \mathbf{f}\|$  does not decrease do
      Solve Eq. (46) for  $1 \leq n \leq N$ 
    end while
    Normalize the basis set and compute the coefficients  $\{\alpha_1, \dots, \alpha_R\}$ 
    Set  $R = R + 1$ 
  end while
end for

```

putational efficiency of the whole method. To avoid this problem, we replace the condition $\|\mathbf{A}\mathbf{p}^R - \mathbf{f}\| < \varepsilon$ with a simpler criterion for convergence, i.e.,

$$\max \left\{ \frac{\|\tilde{\mathbf{p}}_1^R - \mathbf{p}_1^R\|}{\|\mathbf{p}_1^R\|}, \dots, \frac{\|\tilde{\mathbf{p}}_N^R - \mathbf{p}_N^R\|}{\|\mathbf{p}_N^R\|} \right\} \leq \varepsilon_1, \quad (48)$$

where $\{\tilde{\mathbf{p}}_1^R, \dots, \tilde{\mathbf{p}}_N^R\}$ denotes the solution at the previous iteration. Note that the condition (48) involves the computation of N vector norms instead of one N -dimensional tensor norm.

References

- [1] C. Cercignani, *The Boltzmann Equation and Its Applications*, Springer, 1988.
- [2] C. Cercignani, U.I. Gerasimenko, D.Y. Petrina, *Many Particle Dynamics and Kinetic Equations*, 1st edition, Kluwer Academic Publishers, 1997.
- [3] P. Markovich, C. Ringhofer, C. Schmeiser, *Semiconductor Equations*, Springer, 1989.
- [4] F. Moss, P.V.E. McClintock (Eds.), *Noise in Nonlinear Dynamical Systems, vol. 1: Theory of Continuous Fokker–Planck Systems*, Cambridge Univ. Press, 1995.
- [5] F. Moss, P.V.E. McClintock (Eds.), *Noise in Nonlinear Dynamical Systems, vol. 2: Theory of Noise Induced Processes in Special Applications*, Cambridge Univ. Press, 1995.
- [6] F. Moss, P.V.E. McClintock (Eds.), *Noise in Nonlinear Dynamical Systems, vol. 3: Experiments and Simulations*, Cambridge Univ. Press, 1995.
- [7] K. Sobczyk, *Stochastic Differential Equations: With Applications to Physics and Engineering*, Springer, 2001.
- [8] D. Lucor, C.H. Su, G.E. Karniadakis, Generalized polynomial chaos and random oscillators, *Int. J. Numer. Methods Eng.* 60 (3) (2004) 571–596.
- [9] H. Cho, D. Venturi, G.E. Karniadakis, Adaptive discontinuous Galerkin method for response–excitation PDF equations, *SIAM J. Sci. Comput.* 35 (4) (2013) B890–B911.
- [10] D. Venturi, T.P. Sapsis, H. Cho, G.E. Karniadakis, A computable evolution equation for the probability density function of stochastic dynamical systems, *Proc. R. Soc. A* 468 (2012) 759–783.
- [11] J. Li, J.-B. Chen, *Stochastic Dynamics of Structures*, Wiley, 2009.
- [12] M.F. Shlesinger, T. Swean, *Stochastically Excited Nonlinear Ocean Structures*, World Scientific, 1998.
- [13] V.V. Bolotin, *Statistical Methods in Structural Mechanics*, Holden-Day, San Francisco, 1969.
- [14] A.N. Malakhov, A.I. Saichev, Kinetic equations in the theory of random waves, *Radiophys. Quantum Electron.* 17 (5) (1974) 526–534.
- [15] V.I. Klyatskin, *Dynamics of Stochastic Systems*, Elsevier Publishing Company, 2005.
- [16] D. Venturi, G.E. Karniadakis, Convolutionless Nakajima–Zwanzig equations for stochastic analysis in nonlinear dynamical systems, *Proc. R. Soc. A* 470 (2166) (2014) 1–20.
- [17] D. Venturi, G.E. Karniadakis, New evolution equations for the joint response–excitation probability density function of stochastic solutions to first-order nonlinear PDEs, *J. Comput. Phys.* 231 (21) (2012) 7450–7474.
- [18] H. Cho, D. Venturi, G.E. Karniadakis, Statistical analysis and simulation of random shocks in Burgers equation, *Proc. R. Soc. A* 260 (2014) 20140080.
- [19] A.S. Monin, A.M. Yaglom, *Statistical Fluid Mechanics, vol. I: Mechanics of Turbulence*, Dover, 2007.
- [20] A.S. Monin, A.M. Yaglom, *Statistical Fluid Mechanics, vol. II: Mechanics of Turbulence*, Dover, 2007.
- [21] U. Frisch, *Turbulence: The Legacy of A.N. Kolmogorov*, Cambridge University Press, 1995.
- [22] S.B. Pope, Lagrangian PDF methods for turbulent flows, *Annu. Rev. Fluid Mech.* 26 (1994) 23–63.
- [23] D. Nozaki, D.J. Mar, P. Grigg, J.J. Collins, Effects of colored noise on stochastic resonance in sensory neurons, *Phys. Rev. Lett.* 82 (11) (1999) 2402–2405.
- [24] C. Zeng, H. Wang, Colored noise enhanced stability in a tumor cell growth system under immune response, *J. Stat. Phys.* 141 (5) (2010) 889–908.
- [25] A. Fiasconaro, B. Spagnolo, A. Ochab-Marcinek, E. Gudowska-Nowak, Co-occurrence of resonant activation and noise-enhanced stability in a model of cancer growth in the presence of immune response, *Phys. Rev. E* 74 (4) (2006) 041904.
- [26] H. Risken, *The Fokker–Planck Equation: Methods of Solution and Applications*, 2nd edition, Math. Sci. Eng., vol. 60, Springer-Verlag, 1989.
- [27] R.L. Stratonovich, Some Markov methods in the theory of stochastic processes in nonlinear dynamical systems, in: F. Moss, P.V.E. McClintock (Eds.), *Noise in Nonlinear Dynamical Systems, vol. 1*, Cambridge Univ. Press, 1989, pp. 16–68.
- [28] C. Villani, A review of mathematical topics in collisional kinetic theory, in: S. Friedlander, D. Serre (Eds.), *Handbook of Mathematical Fluid Mechanics, vol. 1*, North-Holland, 2002, pp. 71–305.
- [29] B.G. Dostupov, V.S. Pugachev, The equation for the integral of a system of ordinary differential equations containing random parameters, *Automat. Telemekh.* 18 (1957) 620–630 (in Russian).
- [30] R. Zwanzig, Memory effects in irreversible thermodynamics, *Phys. Rev.* 124 (1961) 983–992.
- [31] G. Dimarco, L. Paresci, Numerical methods for kinetic equations, *Acta Numer.* 23 (4) (2014) 369–520.
- [32] R.P. Kanwal, *Generalized Functions: Theory and Technique*, 2nd edition, Birkhäuser, Boston, 1998.
- [33] Y. Yang, C.-W. Shu, Discontinuous Galerkin method for hyperbolic equations involving δ -singularities: negative-order norm error estimates and applications, *Numer. Math.* 124 (2013) 753–781.

- [34] S.B. Pope, Simple models of turbulent flows, *Phys. Fluids* 23 (1) (2011) 011301.
- [35] S.B. Pope, A Monte Carlo method for the PDF equations of turbulent reactive flow, *Combust. Sci. Technol.* 25 (1981) 159–174.
- [36] M. Muradoglu, P. Jenny, S.B. Pope, D.A. Caughey, A consistent hybrid finite-volume/particle method for the PDF equations of turbulent reactive flows, *J. Comput. Phys.* 154 (1999) 342–371.
- [37] L. Valino, A field Monte Carlo formulation for calculating the probability density function of a single scalar in a turbulent flow, *Flow Turbul. Combust.* 60 (2) (1998) 157–172.
- [38] R.O. Fox, *Computational Models for Turbulent Reactive Flows*, Cambridge University Press, 2003.
- [39] G.A. Bird, *Molecular Gas Dynamics and Direct Numerical Simulation of Gas Flows*, Clarendon Press, 1994.
- [40] S. Rjasanow, W. Wagner, *Stochastic Numerics for the Boltzmann Equation*, Springer, 2004.
- [41] F. Filbet, G. Russo, High-order numerical methods for the space non-homogeneous Boltzmann equations, *J. Comput. Phys.* 186 (2003) 457–480.
- [42] Y. Cheng, I.M. Gamba, A. Majorana, C.-W. Shu, A discontinuous Galerkin solver for Boltzmann–Poisson systems in nano devices, *Comput. Methods Appl. Mech. Eng.* 198 (2009) 3130–3150.
- [43] Y. Cheng, I.M. Gamba, A. Majorana, C.-W. Shu, A brief survey of the discontinuous Galerkin method for the Boltzmann–Poisson equations, *SeMA J.* 54 (2011) 47–64.
- [44] B. Cockburn, G.E. Karniadakis, C.-W. Shu, *Discontinuous Galerkin Methods*, *Lect. Notes Comput. Sci. Eng.*, vol. 11, Springer, 2000.
- [45] J.-F. Remacle, J.E. Flaherty, M.S. Shephard, An adaptive discontinuous Galerkin technique with an orthogonal basis applied to compressible flow problems, *SIAM Rev.* 45 (1) (2003) 53–72.
- [46] F. Chinesta, A. Ammar, E. Cueto, Recent advances and new challenges in the use of the proper generalized decomposition for solving multidimensional models, *Comput. Methods Appl. Mech. Eng.* 17 (4) (2010) 327–350.
- [47] G. Leonenko, T. Phillips, On the solution of the Fokker–Planck equation using a high-order reduced basis approximation, *Comput. Methods Appl. Mech. Eng.* 199 (1–4) (2009) 158–168.
- [48] A. Nouy, Proper generalized decompositions and separated representations for the numerical solution of high dimensional stochastic problems, *Comput. Methods Appl. Mech. Eng.* 17 (2010) 403–434.
- [49] A. Nouy, A priori model reduction through proper generalized decomposition for solving time-dependent partial differential equations, *Comput. Methods Appl. Mech. Eng.* 199 (23–24) (2010) 1603–1626.
- [50] D. Montgomery, A BBGKY framework for fluid turbulence, *Phys. Fluids* 19 (6) (1976) 802–810.
- [51] G. Li, S.-W. Wang, H. Rabitz, S. Wang, P. Jaffé, Global uncertainty assessments by high dimensional model representations (HDMR), *Chem. Eng. Sci.* 57 (21) (2002) 4445–4460.
- [52] Z. Gao, J.S. Hesthaven, On ANOVA expansions and strategies for choosing the anchor point, *Appl. Math. Comput.* 217 (7) (2010) 3274–3285.
- [53] Y. Cao, Z. Chen, M. Gunzburger, ANOVA expansions and efficient sampling methods for parameter dependent nonlinear PDEs, *Int. J. Numer. Anal. Model.* 6 (2009) 256–273.
- [54] Z. Zhang, M. Choi, G.E. Karniadakis, Error estimates for the ANOVA method with polynomial chaos interpolation: tensor product functions, *SIAM J. Sci. Comput.* 34 (2) (2012) 1165–1186.
- [55] A. Ammar, B. Mokdad, F. Chinesta, R. Keunings, A new family of solvers for some classes of multidimensional partial differential equations encountered in kinetic theory modelling of complex fluids: Part II: Transient simulation using space–time separated representations, *J. Non-Newton. Fluid Mech.* 144 (2) (2007) 98–121.
- [56] A. Nouy, O.P.L. Maître, Generalized spectral decomposition for stochastic nonlinear problems, *J. Comput. Phys.* 228 (2009) 202–235.
- [57] G. Beylkin, M.J. Mohlenkamp, Algorithms for numerical analysis in high dimensions, *SIAM J. Sci. Comput.* 26 (6) (2005) 2133–2159.
- [58] G. Beylkin, J. Garcke, M.J. Mohlenkamp, Multivariate regression and machine learning with sums of separable functions, *SIAM J. Sci. Comput.* 31 (3) (2009) 1840–1857.
- [59] A. Doostan, G. Iaccarino, A least-squares approximation of partial differential equations with high-dimensional random inputs, *J. Comput. Phys.* 228 (12) (2009) 4332–4345.
- [60] I.M. Sobol, Global sensitivity indices for nonlinear mathematical models and their Monte Carlo estimates, *Math. Comput. Simul.* 55 (2001) 271–280.
- [61] A. Saltelli, K. Chan, M. Scott, *Sensitivity Analysis*, John Wiley, 2000.
- [62] D. Venturi, M. Choi, G.E. Karniadakis, Supercritical quasi-conduction states in stochastic Rayleigh–Bénard convection, *Int. J. Heat Mass Transf.* 55 (13–14) (2012) 3732–3743.
- [63] X. Wan, G.E. Karniadakis, An adaptive multi-element generalized polynomial chaos method for stochastic differential equations, *J. Comput. Phys.* 209 (2) (2005) 617–642.
- [64] X. Yang, M. Choi, G.E. Karniadakis, Adaptive ANOVA decomposition of stochastic incompressible and compressible fluid flows, *J. Comput. Phys.* 231 (2012) 1587–1614.
- [65] M. Griebel, Sparse grids and related approximation schemes for higher dimensional problems, in: L.M. Pardo, A. Pinkus, E. Süli, M.J. Todd (Eds.), *Foundations of Computational Mathematics*, vol. 331, Santander 2005, Cambridge University Press, 2006, pp. 106–161.
- [66] H. Rabitz, Ö.F. Aliş, J. Shorter, K. Shim, Efficient input–output model representations, *Comput. Phys. Commun.* 117 (1–2) (1999) 11–20.
- [67] Z. Zhang, M. Choi, G.E. Karniadakis, Anchor points matter in ANOVA decomposition, in: E. Ronquist, J. Hesthaven (Eds.), *Proceedings of ICOSAHOM'09*, Springer, 2010.
- [68] J. Foo, G.E. Karniadakis, Multi-element probabilistic collocation method in high dimensions, *J. Comput. Phys.* 229 (2010) 1536–1557.
- [69] H.-K. Rhee, R. Aris, N.R. Amundson, *First-order Partial Differential Equations*, vol. 1: Theory and Applications of Single Equations, Dover, 2001.
- [70] E.N. Lorenz, Predictability – a problem partly solved, in: *ECMWF Seminar on Predictability: vol. 1*, Reading, 1996, pp. 1–18.
- [71] A. Karimi, M.R. Paul, Extensive chaos in the Lorenz-96 model, *Chaos* 20 (4) (2010) 043105.
- [72] P.C. Martin, E.D. Siggia, H.A. Rose, Statistical dynamics of classical systems, *Phys. Rev. A* 8 (1973) 423–437.
- [73] B. Jouvét, R. Phythian, Quantum aspects of classical and statistical fields, *Phys. Rev. A* 19 (3) (1979) 1350–1355.
- [74] R. Phythian, The functional formalism of classical statistical dynamics, *J. Phys. A, Math. Gen.* 10 (5) (1977) 777–788.
- [75] M. Waclawczyk, N. Staffolani, M. Oberlack, A. Rosteck, M. Wilczek, R. Friedrich, Statistical symmetries of the Lundgren–Monin–Novikov hierarchy, *Phys. Rev. E* 90 (2014) 013022.
- [76] T.S. Lundgren, Distribution functions in the statistical theory of turbulence, *Phys. Fluids* 10 (5) (1967) 969–975.
- [77] N. Halko, P.-G. Martinsson, J.A. Tropp, Finding structure with randomness: probabilistic algorithms for constructing approximate matrix decompositions, *SIAM Rev.* 53 (2) (2011) 217–288.
- [78] D.J. Biagioni, D. Beylkin, G. Beylkin, Randomized interpolative decomposition of separated representations, *J. Comput. Phys.* 281 (2015) 116–134.
- [79] I.V. Oseledets, Tensor–train decomposition, *SIAM J. Sci. Comput.* 33 (5) (2011) 2295–2317.
- [80] J.S. Hesthaven, S. Gottlieb, D. Gottlieb, *Spectral Methods for Time-Dependent Problems*, Cambridge Univ. Press, 2007.